JGR Planets

RESEARCH ARTICLE
10.1029/2022JE007185

Special Section:
The Curiosity rover's investigation of Glen Torridon and the surrounding area

The Curiosity Rover's Exploration of Glen Torridon, Gale Crater, Mars: An Overview of the Campaign and Scientific Results

Kristen A. Bennett[1], Valerie K. Fox[2,3], Alex Bryk[4], William Dietrich[4], Christopher Fedo[5], Lauren Edgar[1], Michael T. Thorpe[6], Amy J. Williams[7], Gregory M. Wong[8], Erwin Dehouck[9], Amy McAdam[10], Brad Sutter[11,12], Maëva Millan[10,13,14], Steven G. Banham[15], Candice C. Bedford[12,16], Thomas Bristow[17], Abigail Fraeman[18], Ashwin R. Vasavada[18], John Grotzinger[3], Lucy Thompson[19], Catherine O'Connell-Cooper[19], Patrick Gasda[20], Amanda Rudolph[21], Robert Sullivan[22], Ray Arvidson[23], Agnes Cousin[24], Briony Horgan[21], Kathryn M. Stack[18], Allan Treiman[16], Jennifer Eigenbrode[10], and Gwénaël Caravaca[24]

[1]Astrogeology Science Center, U.S. Geological Survey, Flagstaff, AZ, USA, [2]Department of Earth and Environmental Sciences, University of Minnesota, Minneapolis, MN, USA, [3]Division of Geologic and Planetary Sciences, California Institute of Technology, Pasadena, CA, USA, [4]Department of Earth and Planetary Science, University of California, Berkeley, Berkeley, CA, USA, [5]Department of Earth and Planetary Sciences, University of Tennessee, Knoxville, TN, USA, [6]Texas State University, JETS, NASA Johnson Space Center, Houston, TX, USA, [7]Department of Geological Sciences, University of Florida, Gainesville, FL, USA, [8]Department of Geosciences, The Pennsylvania State University, University Park, PA, USA, [9]Université de Lyon, UCBL, ENSL, UJM, CNRS, LGL-TPE, Villeurbanne, France, [10]NASA Goddard Space Flight Center, Greenbelt, MD, USA, [11]Jacobs Technology, Houston, TX, USA, [12]NASA Johnson Space Center, Houston, TX, USA, [13]Department of Biology, Georgetown University, Washington, DC, USA, [14]Laboratoire Atmosphère, Observations Spatiales (LATMOS), LATMOS/IPSL, UVSQ Université Paris-Saclay, Sorbonne Université, CNRS, Guyancourt, France, [15]Department of Earth Sciences and Engineering, Imperial College London, London, UK, [16]Lunar and Planetary Institute, Houston, TX, USA, [17]NASA Ames Research Center, Moffett Field, CA, USA, [18]Jet Propulsion Laboratory, California Institute of Technology, Pasadena, CA, USA, [19]Planetary and Space Science Centre, University of New Brunswick, Fredericton, NB, Canada, [20]Los Alamos National Laboratory, Los Alamos, NM, USA, [21]Earth Atmosphere and Planetary Science, Purdue University, West Lafayette, IN, USA, [22]CCAPS, Cornell University, Ithaca, NY, USA, [23]Department of Earth and Planetary Sciences, Washington University in St. Louis, St. Louis, MO, USA, [24]IRAP, Université de Toulouse, CNRS, CNES, Toulouse, France

Abstract The Mars Science Laboratory rover, *Curiosity*, explored the clay mineral-bearing Glen Torridon region for 1 Martian year between January 2019 and January 2021, including a short campaign onto the Greenheugh pediment. The Glen Torridon campaign sought to characterize the geology of the area, seek evidence of habitable environments, and document the onset of a potentially global climatic transition during the Hesperian era. *Curiosity* roved 5 km in total throughout Glen Torridon, from the Vera Rubin ridge to the northern margin of the Greenheugh pediment. *Curiosity* acquired samples from 11 drill holes during this campaign and conducted the first Martian thermochemolytic-based organics detection experiment with the Sample Analysis at Mars instrument suite. The lowest elevations within Glen Torridon represent a continuation of lacustrine Murray formation deposits, but overlying widespread cross bedded sandstones indicate an interval of more energetic fluvial environments and prompted the definition of a new stratigraphic formation in the Mount Sharp group called the Carolyn Shoemaker formation. Glen Torridon hosts abundant phyllosilicates yet remains compositionally and mineralogically comparable to the rest of the Mount Sharp group. Glen Torridon samples have a great diversity and abundance of sulfur-bearing organic molecules, which are consistent with the presence of ancient refractory organic matter. The Glen Torridon region experienced heterogeneous diagenesis, with the most striking alteration occurring just below the Siccar Point unconformity at the Greenheugh pediment. Results from the pediment campaign show that the capping sandstone formed within the Stimson Hesperian aeolian sand sea that experienced seasonal variations in wind direction.

Plain Language Summary The Mars Science Laboratory rover, *Curiosity*, explored a valley called Glen Torridon on the lower slopes of a sedimentary mountain within Gale crater, Mars, between January 2019 and January 2021. The rocks within this shallow valley are part of a sequence of rock layers whose mineral composition could imply a transition from a wetter to drier environment more than 3 billion years ago. This

Key Points:

- Sedimentary facies within Glen Torridon record a transition from low-energy lacustrine mudstones to higher-energy fluvial sandstones
- Glen Torridon hosts the highest clay mineral abundances observed thus far by Mars Science Laboratory (MSL) while remaining in family with the Mount Sharp group
- Glen Torridon drill samples contain the greatest diversity of organic compounds yet detected by the MSL mission

Supporting Information:

Supporting Information may be found in the online version of this article.

Correspondence to:

K. A. Bennett,
kbennett@usgs.gov

Citation:

Bennett, K. A., Fox, V. K., Bryk, A., Dietrich, W., Fedo, C., Edgar, L., et al. (2023). The Curiosity rover's exploration of Glen Torridon, Gale crater, Mars: An overview of the campaign and scientific results. *Journal of Geophysical Research: Planets*, *128*, e2022JE007185. https://doi.org/10.1029/2022JE007185

Received 18 JAN 2022
Accepted 12 MAY 2022

paper reports on the exploration campaign designed to understand the local geology, document evidence of past climate change, and investigate if the ancient environments may have been amenable to biological activity. *Curiosity* found that many rocks were deposited in the bottom of a lake, but also that river deposits occur frequently in this area, suggesting that the environmental conditions changed through time. *Curiosity* observed evidence for multiple cycles of water interacting with the sediments that chemically changed the elemental and mineralogical compositions of the rock layers. *Curiosity* collected 11 drill holes over the course of the campaign and found abundant clay minerals, as predicted, as well as a wide variety of organic molecules, suggesting that the ancient environment contained many of the necessary conditions to support life.

1. Introduction

Orbital and in-situ observations support a complex history of aqueous activity within Gale crater (e.g., Ehlmann & Buz, 2015; Fraeman et al., 2016; Hurowitz et al., 2017; Le Deit et al., 2013; Palucis et al., 2016; Rampe et al., 2017; Yen et al., 2017), and strata within Mount Sharp (formally Aeolis Mons, the ∼5 km tall central sedimentary mound, Figure 1) host mineralogical and morphological evidence for possibly globally significant climatic changes (Anderson & Bell, 2010; Milliken et al., 2010). Prior to the Mars Science Laboratory (MSL) *Curiosity* rover's landing in 2012, orbital analyses using Compact Reconnaissance Imaging Spectrometer for Mars (CRISM; Murchie et al., 2007) data detected Mg-sulfate bearing layered outcrops overlying Fe-smectite bearing strata; this sequence suggests the rock record documents a significant environmental change from wetter to more arid conditions (Milliken et al., 2010; Thomson et al., 2011). Such stratigraphic relationships are detected in numerous locations across Mars, which indicates that in-situ exploration of the transition in Mount Sharp could have implications for global climate shifts (Bibring et al., 2006; Grotzinger & Milliken, 2012). The presence of smectite clay minerals also suggests both a circumneutral aqueous environment and a possible taphonomic window where organic molecules might have been concentrated and/or preserved. Smectites, particularly, when present at the time of sedimentary deposition, can sometimes have high organic preservation potential (Summons et al., 2011). The mineral detections on the northwest slopes of Mount Sharp are also distinctive because much of Gale crater is spectrally bland as a result of dust and sand cover (Seelos et al., 2014; Thomson et al., 2011). Therefore, the region associated with CRISM smectite detections, now called Glen Torridon, became a prime exploration goal for the *Curiosity* rover where the MSL mission could test hypotheses about the globally observed climactic shift and ancient habitability (Grotzinger et al., 2012).

The *Curiosity* rover explored the Glen Torridon region (Figure 2) during a campaign that started in January 2019 (sol 2300) after descending the south side of Vera Rubin ridge. The rover explored this area until January 2021 (sol 3072) and obtained a suite of textural, sedimentological, geochemical, and mineralogical data that has been used to interpret the geologic history of the region. In this manuscript we describe *Curiosity*'s traverse through the clay-bearing Glen Torridon and the summarize the primary findings from this key study region.

2. Background

2.1. Geologic Context of Gale Crater

Gale crater is located at the global dichotomy boundary between the southern highlands and northern lowlands. Gale crater's floor is the lowest location for over 1,000 km in either direction along the great dichotomy and the lowest locations for >500 km to the south. Over its history, cycles of sedimentation and erosion filled and then excavated the crater, leaving a lengthy record of both surface and subsurface aqueous environments, making Gale a valuable exploration site to better constrain both the history of water and the habitability of ancient Mars (Wray, 2013).

Prior to arriving at Glen Torridon, *Curiosity* traversed from its landing site on the floor of Gale crater (Aeolis Palus) to the lower flanks of Mount Sharp (Figure 1). Thus far, detailed sedimentological and stratigraphic analysis has resulted in the definition of three stratigraphic groups: The Bradbury group on the crater floor, the Mount Sharp group in Aeolis Mons, and the Siccar Point group that unconformably overlies the Mount Sharp group (i.e., Stack et al., 2019). The Bradbury group is comprised of fluvial-deltaic deposits with intervals of lacustrine mudstones. The first phyllosilicate minerals detected by *Curiosity* in Gale crater were observed the Yellowknife Bay formation, one such lacustrine deposit in the Bradbury group (Grotzinger et al., 2014; Vaniman et al., 2014).

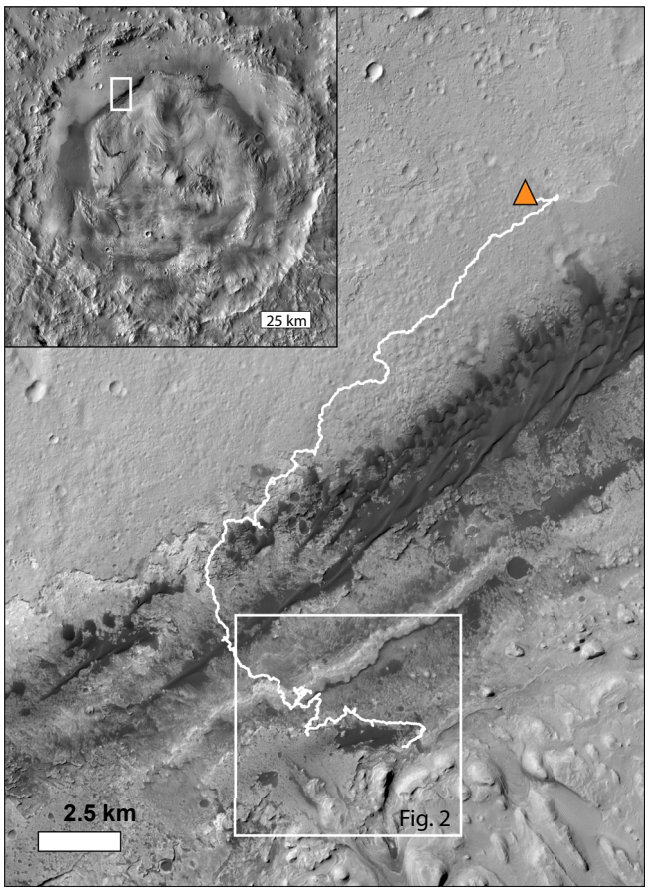

Figure 1. Upper left inset: THEMIS-VIS Band 3 mosaic of Gale crater (Bennett, Hill, et al., 2018). The white box shows location of the rest of the figure. Main figure: CTX image (D01_027557_1754_XN_04S222W) showing the Curiosity rover's traverse (white line) through sol 3149. The triangle shows the landing site. The white box shows the location of Figure 2 and contains the study area of this campaign.

Lower Mount Sharp group strata are primarily dominated by lake and lake margin mudstone deposits (Edgar et al., 2020; Grotzinger et al., 2015; Gwizd et al., 2020; Rivera-Hernández et al., 2020; Stack et al., 2019) that have been defined as part of the Murray formation. The Murray formation is divided into seven lithostratigraphic members based on subtle changes in lithology and facies associations (Edgar et al., 2020; Fedo et al., 2018; Stack et al., 2019) (Figure 3), but are for the most part dominated by finely laminated mudstones punctuated with sandstone deposits. The Murray formation is more than 300 m thick, which implies that a lacustrine environment was present in Gale crater for an extended period of time (likely in excess of 10^6 years; Edgar et al., 2020). Siccar Point group rocks unconformably overlie the Mount Sharp group and represent the preserved expression of migrating sand dunes within a larger dune field that were deposited and lithified after the formation and subsequent erosion of the Mount Sharp central mound (Banham et al., 2018, 2021; Bedford et al., 2020). The rover has encountered several exposures of the Stimson formation aeolian sandstone deposits that form resistant caps overlying Murray formation deposits at the Emerson and Naukluft plateaus and the Murray Buttes.

Immediately prior to the Glen Torridon campaign, *Curiosity* completed an extensive investigation of Vera Rubin ridge (Fraeman, Edgar, et al., 2020), which exhibits strong hematite signatures in orbital data sets (Fraeman, Edgar, et al., 2020; Fraeman, Johnson, et al., 2020; Fraeman et al., 2016). *Curiosity* measurements demonstrated Vera Rubin ridge contains abundant iron oxides, including hematite, and low abundances of phyllosilicates (Rampe, Blake, et al., 2020). The distinct geomorphic expression and mineralogy of Vera Rubin ridge compared to contiguous Murray formation facies are interpreted to be a result of multiple diagenetic events that cemented or recrystallized the sediments such that they became erosion-resistant and formed a ridge (Fraeman, Johnson, et al., 2020; L'Haridon et al., 2020). Color variations within the ridge (primarily red vs. gray mudstones) were observed to crosscut stratigraphy and therefore were also interpreted to be a result of diagenesis (Edgar et al., 2020; L'Haridon et al., 2020). Two stratigraphic members, Pettegrove Point and Jura, outcrop on Vera Rubin ridge, both of which are interpreted to be a continuation of the primarily lacustrine Murray formation.

2.2. Glen Torridon Background

Glen Torridon is an asymmetric trough that extends laterally ~5 km ENE-WSW. It is bounded to the north by Vera Rubin ridge (Fraeman, Edgar, et al., 2020) and to the south by both the Greenheugh pediment and the steepening slopes of the sulfate unit (Figures 2 and 4). The region has previously been called the Phyllosilicate Trough (Anderson & Bell, 2010), phyllosilicate layers (Milliken et al., 2010), the Phyllosilicate Unit (Fraeman et al., 2016) and the clay-bearing unit (Bennett, Fox, et al., 2018; Fox et al., 2018), all based on the orbitally derived identification of smectites. The majority of *Curiosity*'s traverse through this area occurred in the "Torridon" quadrangle, which was defined in the geologic map created by the MSL team before arrival (Grotzinger et al., 2014). Torridon is a small village in the northwest highlands of Scotland in a region key to understanding the geologic history and origin of life, and science targets within this quadrangle on Mars, including Glen Torridon, are informally named according to this theme.

Prior to *Curiosity*'s landing, the Glen Torridon region was identified as a region of interest because of the distinct smectite signatures present across the trough in reflectance spectral data from the CRISM instrument that were not detected elsewhere within the crater (Milliken et al., 2010). Smectites are identified in near-infrared reflectance spectra by the occurrence of Al-OH, Fe-OH and/or Mg-OH bending and stretching combination absorptions around 2.20, 2.28, and 2.31 μm, respectively, together with hydration absorptions at 1.4 and 1.9 μm (Bishop et al., 2008; Fox et al., 2021). Spectra from Glen Torridon display absorptions at 1.9, 2.24, and 2.28 μm, indicating

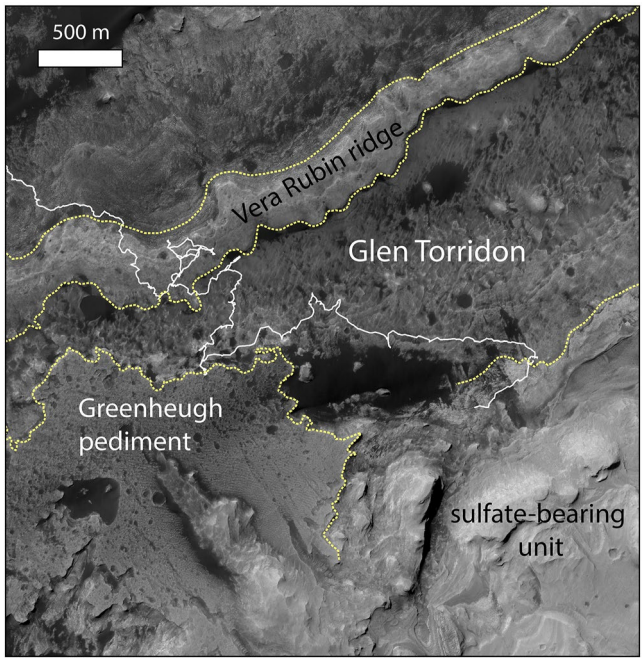

Figure 2. HiRISE image (ESP_053732_1750) showing the geomorphic features in and around the study area. Glen Torridon is a trough that is bounded to the north by Vera Rubin ridge and to the south by the Greenheugh pediment and the sulfate-bearing unit. Yellow dashed lines highlight the boundaries between these geomorphic features and the white line shows the traverse path.

the presence of ferric smectite (nontronite) with some aluminum substitution (Ehlmann & Buz, 2015; Milliken et al., 2010). Initial orbital studies proposed that the outcrops could be distinct phyllosilicate-bearing strata within the Mt. Sharp stratigraphy (Anderson & Bell, 2010; Fraeman et al., 2016), or an unconformable deposit of phyllosilicate-cemented sandstones that was deposited after the formation of Mount Sharp (Milliken et al., 2014). It was also thought that the strata might be uniquely rich in phyllosilicates as compared to the surrounding area. However, results from *Curiosity* demonstrate that smectites are present, in some cases comprising >25 wt%, in many of the samples that have been analyzed thus far from both the crater floor and Mount Sharp (Bristow et al., 2018; Rampe, Blake, et al., 2020; Rampe et al., 2017; Tu et al., 2021; Vaniman et al., 2014). This raised the question of why smectites at Gale crater are detectable from orbit only within Glen Torridon.

In advance of *Curiosity*'s arrival, Glen Torridon outcrops were mapped into three informal units—"smooth clay-bearing," "fractured clay-bearing," and an "fractured intermediate unit"—(Figure 4) using both spectral and geomorphic data from CRISM and HiRISE (McEwen et al., 2007). The smectite spectral signatures are most clear in the northern, lowest-elevation portion of the trough and are detected across both smooth textured surfaces that are more common to the north (the smooth clay-bearing unit) and fractured bedrock outcrops that are more common to the south (the fractured clay-bearing unit). The smooth textured regions are also punctuated by NE/SW trending ridges that were hypothesized to be either lithified sand dunes (Milliken et al., 2014) or erosional features such as periodic bedrock ridges (Montgomery et al., 2012). The ridges also occur in the regions with fractured bedrock but are less well defined in these areas. Third, the generically named "fractured intermediate unit" is mapped along the southern border of Glen Torridon, between the smooth and fractured clay-bearing units and the Greenheugh pediment and the Mg-sulfate bearing unit to the south. The unit is predominately fractured bedrock outcrops, but the spectral signatures from these strata are non-unique and best characterized by a steep red slope between 1 and 1.6 μm with variable metal-OH features (Fraeman et al., 2016).

The Greenheugh pediment is a fan-shaped feature situated at the base of Gediz Vallis and its capping unit overlies the clay-bearing strata of the Glen Torridon region (Figure 2). The northern edge of the pediment was investigated during the Glen Torridon campaign from sol 2691 to sol 2734. From orbit, the Greenheugh pediment capping unit does not show any spectral signatures of hydrated minerals, but has a similar high thermal inertia (Fraeman et al., 2016) to the aeolian sandstones of the Stimson formation that were investigated farther downslope at the Emerson plateau, Naukluft plateau, and Murray Buttes (Banham et al., 2018, 2021; Bedford et al., 2020; Fraeman et al., 2016). The Stimson formation overlies the Siccar Point unconformity, which records the termination of net sediment accretion and building of Mt Sharp and the transition to net erosion of the north face of the mountain, which is still active today under hyper-arid conditions (Banham et al., 2018, 2021; Bedford et al., 2020). While surface water was likely rare after Stimson deposition, diagenetic cement and aqueous alteration in the Stimson sandstones suggest that liquid subsurface water was present even well after Mt Sharp construction and erosion, indicating the possibility of continued and sustained habitable conditions (Banham et al., 2018, 2021; Bedford et al., 2020).

2.3. Stratigraphic Context of Glen Torridon

For context throughout the rest of this report, we summarize the stratigraphic model developed for Glen Torridon here (Figure 3). Glen Torridon strata represent a continuation of the Mount Sharp group, with the base of the sedimentary succession in Glen Torridon stratigraphically equivalent to strata that outcrop in Vera Rubin ridge (see cross-section shown in Figure 3b). Rocks within Glen Torridon are mapped into three stratigraphic members: Jura, a predominately fine-grained mudstone that also outcrops in Vera Rubin ridge (Edgar et al., 2020), Knockfarril

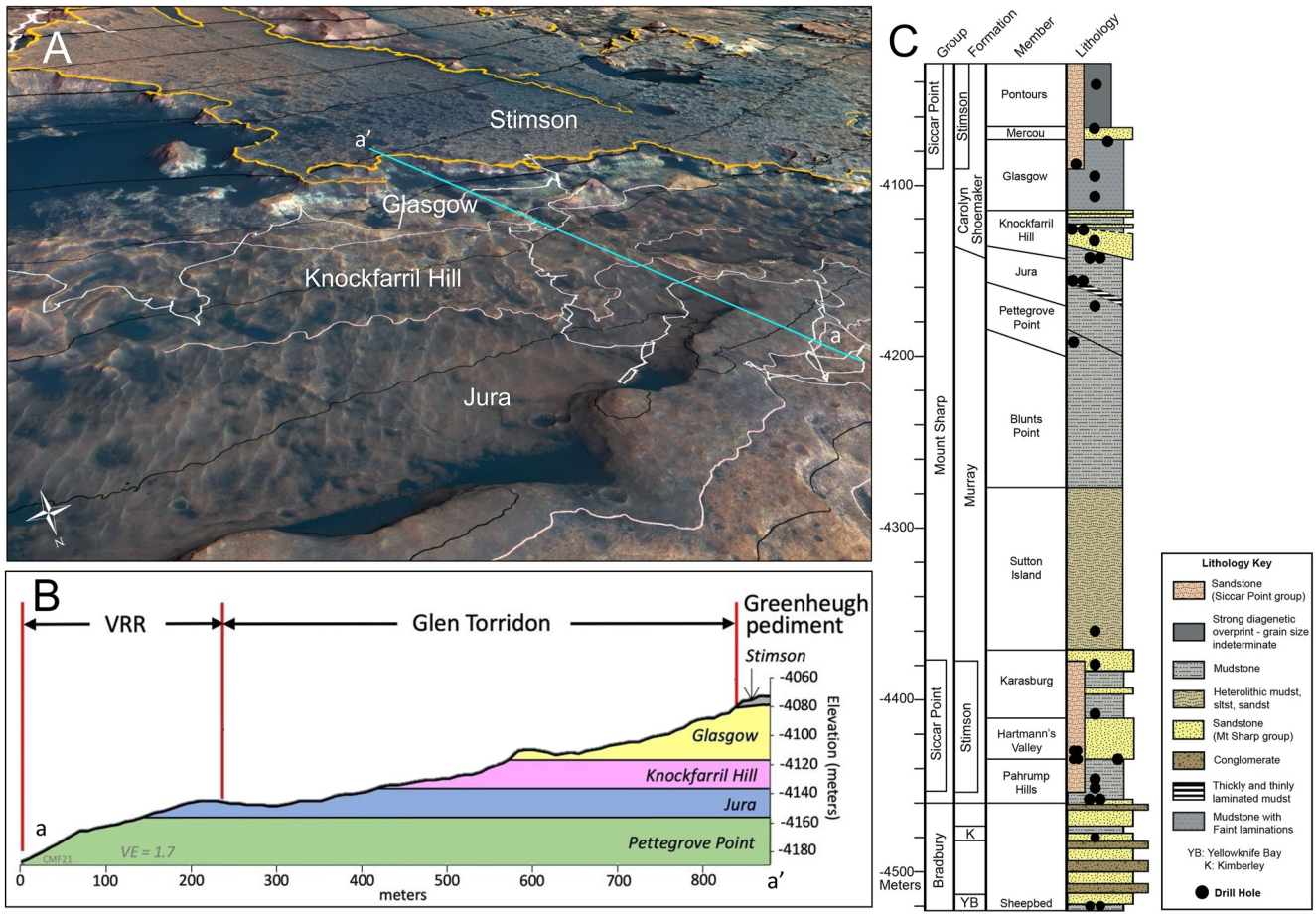

Figure 3. (a) Three-dimensional view of the Glen Torridon area showing the stratigraphic units that outcrop here. The white line is the rover traverse. Pink lines show the boundaries between the stratigraphic members in the Mount Sharp group. The orange line shows the extent of the Siccar Point group. The blue line shows the location of the cross section shown in panel (b). (b) Cross section showing the stratigraphic members in Glen Torridon and the surrounding area, including Vera Rubin ridge (labeled VRR in the figure). The extent of Glen Torridon, Vera Rubin ridge, and the Greenheugh pediment is demonstrated by the red lines. Note that the Jura member outcrops in both Glen Torridon and Vera Rubin ridge. Adapted from Fedo et al. (2022). (c) The composite stratigraphic column of Gale crater strata characterized by Curiosity. The stratigraphic column is adapted from Fedo et al. (2022).

Hill, which is dominated by cross-bedded sandstones (Caravaca et al., 2022; Fedo et al., 2022), and Glasgow, which exhibits a variety of diagenetic textures overprinting laminated mudstones, particularly in locations adjacent to the Greenheugh pediment (Dehouck et al., 2022; Gasda et al., 2022; O'Connell-Cooper et al., 2022). The Jura member is the uppermost member of the Murray formation, and the Knockfarril Hill crossbedded sandstones are the lowermost member of the Carolyn Shoemaker formation (Fedo et al., 2022). The Carolyn Shoemaker formation marks a transition from the generally low-energy lacustrine depositional environment of the Murray formation (Edgar et al., 2020; Fedo et al., 2022) to the presence of fluvial deposits in a lake margin environment (Caravaca et al., 2022), as evidenced by the greater occurrence of cross-bedded sandstones.

3. Campaign Goals

The overarching goal of the MSL mission is to explore the habitability of Mars through investigations of the stratigraphic record in Gale crater (Grotzinger et al., 2012). Related to this goal, the mission is focused on characterizing the geology of Mars, including the past role of water, and understanding the evolution of the atmosphere and climate (Grotzinger et al., 2012). The Glen Torridon region represents a unique opportunity to characterize an important, possibly global, climatic transition that is hypothesized to be recorded in the Mount Sharp strata. Characterizing this area can lead to an improved understanding of the geology of Gale crater and past aqueous and atmospheric processes. Therefore, the MSL science team defined three overarching questions and experimental

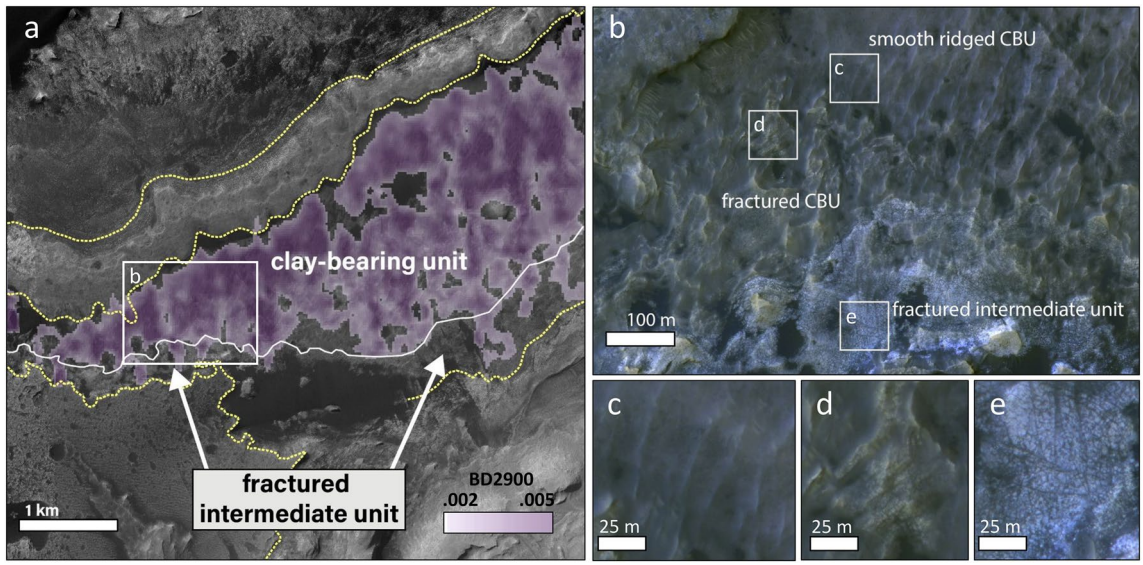

Figure 4. Prior to in-situ exploration, Glen Torridon was divided into the smooth, ridged clay-bearing unit, the fractured clay-bearing unit, and the fractured intermediate unit based on orbital morphology, textures, and mineralogy. (a) Compact Reconnaissance Imaging Spectrometer for Mars (CRISM) smectite parameter map (Background: grayscale Gale orthophoto mosaic from Calef and Parker (2016)). Purple shaded areas show locations of enhanced smectite signatures, with darker shades of purple exhibiting stronger signatures (CRISM observation FRT0000B6F1_07_IF165L_TRR3, 2.9 μm band depth as processed in He et al. (2022)). Dashed yellow lines show geomorphic boundaries from Figure 2. White line shows the rough boundary between the clay-bearing unit and the fractured intermediate unit that does not exhibit clear enhanced smectite signatures. White box shows the location of panel (b). (b) HiRISE color image (ESP_060840_1750) showing the three orbitally defined sub-units within Glen Torridon. (c) Smooth, ridged clay-bearing unit. (d) Fractured clay-bearing unit. (e) Fractured intermediate unit.

tests that centered around characterizing the phyllosilicate-bearing deposits outcropping in Glen Torridon as indicators of past aqueous processes using its instrumental payload (Table 1).

Campaign question 1: *What is the stratigraphic context of rocks exposed in Glen Torridon, and what primary depositional processes are recorded in the strata?* Glen Torridon's geomorphic expression as a topographic low on the slopes of Mount Sharp makes interpreting how the strata fit into the Mount Sharp stratigraphy with orbital data sets challenging (Fraeman et al., 2016). The physical boundary between Vera Rubin ridge terrain and Glen Torridon terrain is a scarp, and the spectral properties of Vera Rubin ridge and Glen Torridon are also markedly different, which could suggest that the ridge units are distinct and stratigraphically above those in Glen Torridon (Fraeman et al., 2016). On the other hand, the Glen Torridon region is gently sloping up Mount Sharp such that Glen Torridon strata also occur at equal and higher elevations than Vera Rubin ridge strata. This geometry, plus the uncertainty related to the dip of the units, means that the stratigraphic relationship between Vera Rubin ridge and Glen Torridon was not well constrained from orbital data sets (Fraeman et al., 2016). The campaign also

Table 1
Curiosity Rover Payload Instruments Used to Address Glen Torridon Science Objectives

Remote sensing instruments		
Mast Cameras	Mastcam	Bell et al. (2017) and Malin et al. (2017)
Chemistry and Camera	ChemCam	Maurice et al. (2012) and Wiens et al. (2012)
Dynamic Albedo of Neutrons	DAN	Mitrofanov et al. (2012) and Sanin et al. (2015)
Arm instruments		
Mars Hand Lens Imager	MAHLI	Edgett et al. (2012)
Alpha-Particle X-Ray Spectrometer	APXS	Gellert et al. (2015)
Laboratory instruments		
Chemistry and Mineralogy	CheMin	Blake et al. (2012)
Sample Analysis at Mars	SAM	Mahaffy et al. (2012)

addressed whether the rocks of Glen Torridon represent a continuation of the lacustrine Murray formation or if there is a record of change in depositional processes.

Campaign question 2: *How did post-depositional processes contribute to the geologic history of the region?* Diagenesis plays a key role throughout the geologic history of Gale crater, in particular the formation and preservation of Vera Rubin ridge, and the Glen Torridon campaign sought to identify and distinguish primary depositional and diagenetic processes. This goal particularly related to the phyllosilicates predicted to be present in the region; before in-situ exploration in Gale crater, most phyllosilicates on Mars were presumed to be formed in Noachian aged terrains (Bibring et al., 2005; Ehlmann et al., 2011). *Curiosity* rover measurements in Yellowknife Bay and multiple sites throughout the Murray formation began to suggest that smectites could have formed in the Hesperian-aged lake surface environments (Bristow et al., 2015, 2018; Mangold et al., 2019; Vaniman et al., 2014). Findings from the Vera Rubin ridge campaign suggest post-depositional, diagenetic phyllosilicate formation and recrystallization, perhaps even further extending the aqueous alteration timeline (Bristow et al., 2021; Rampe, Bristow, et al., 2020). The clay-mineral-rich strata in Glen Torridon were hypothesized to be an ideal region to investigate ideas about where and how clay minerals in the lacustrine Murray formation were formed. The campaign also sought to answer questions about the origin and formation processes of the modern landscape features, particularly the NE/SW linear ridges. In-situ observations could test if these structures were preserved aeolian bedforms or erosional constructs.

Campaign question 3: *What are the implications of depositional and diagenetic conditions recorded within Glen Torridon rocks for habitability? How do the lithologies and geological history of this area impact the preservation of organic molecules?* On Earth, clay-mineral-rich strata frequently have high preservation potential for organic material and can be indicators of past habitable environments and biological communities (Johnson et al., 2020; Summons et al., 2011; Williams et al., 2019). Therefore, Glen Torridon was specifically identified early on by the MSL mission as a high priority region in which to search for organic molecules and potential biomarkers and to better understand the past habitability and biological potential of Gale crater. The Sample Analysis at Mars (SAM) instrument suite (Mahaffy et al., 2012) has been specifically designed to extract, separate, and detect organic molecules by pyrolysis coupled to gas chromatography mass spectrometry (GCMS). In addition, the SAM instrument carries two reagents: the *N*-methyl-*N*-(*tert*-butyldimethylsilyl) trifluoroacetamide (MTBSTFA) and tetramethylammonium hydroxide (TMAH), to conduct "wet chemistry" derivatization and thermochemolysis experiments, respectively. These wet chemistry techniques allow the extraction of polar and refractory organic molecules that are difficult to detect using standard SAM-GCMS analyses. Based on laboratory experiments on Martian analogs, the MTBSTFA (Millan et al., 2018) and TMAH wet chemistry experiments (Williams et al., 2019) were expected to optimally liberate organic molecules preserved in clay-bearing mineral assemblages. The MTBSTFA technique was first tested on a sample of the Bagnold dune field and helped optimize the wet chemistry sequences to be used on the Glen Torridon samples (Millan et al., 2021).

Greenheugh Pediment Exploration Campaign: A preliminary study to examine the Greenheugh pediment aimed to understand the stratigraphy of the sedimentary rocks which cap the pediment surface and explore evidence for erosional processes that generated the pediment surface on which the sediment cap was then deposited. The capping unit was hypothesized to lie unconformably on top of the eroded Mount Sharp group, with implications for the timing of the erosion of Mount Sharp. This excursion was also an opportunity to further investigate the contact between the Mt Sharp group and the Siccar Point group.

4. Glen Torridon Exploration Narrative

4.1. Defining the Traverse

Curiosity investigated the Glen Torridon region from January 2019 until January 2021 (sols 2300–3072). By the conclusion of the Glen Torridon exploration campaign on sol 3072, *Curiosity* drove 24.9 km and ascended ~430 m up strata on the northwest slopes of Mount Sharp (Figure 1).

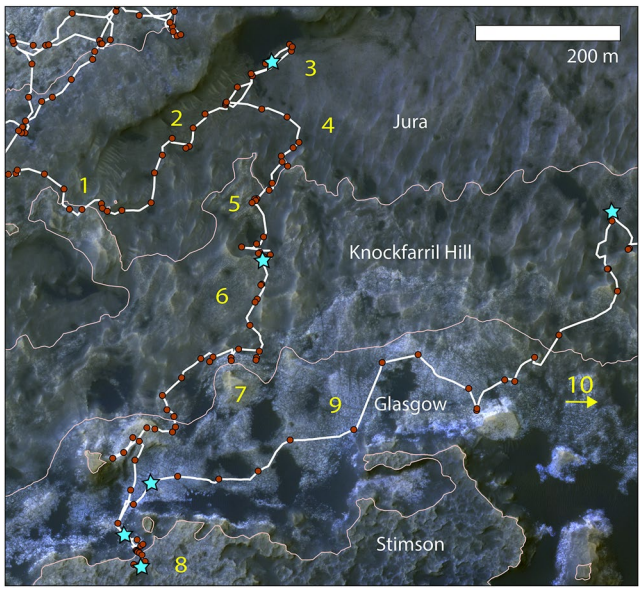

Figure 5. Curiosity's traverse area within Glen Torridon. The white line is the rover traverse path and the red circles are stops along the traverse. The numbers correspond to the 10 waypoints defined in Section 4.1 (HiRISE image ESP_060840_1750). Stars indicate drill sample locations. The stratigraphic members are labeled, and the member boundaries are denoted by the pink lines.

The traverse through Glen Torridon was defined by several waypoints identified by the science team in response to the overarching science questions described above (Figure 5). The following waypoints (numbers match the labels shown in Figure 5) were used to define a preliminary traverse:

1. *Entrance to Glen Torridon region:* The boundary between Vera Rubin ridge and Glen Torridon is a steep cliff face that for the most part is not traversable by a rover. This waypoint marks the safest location to descend into Glen Torridon from Vera Rubin ridge and necessarily defined the start of the traverse within Glen Torridon.
2. *Vera Rubin ridge imaging:* The rover traversed east-northeast along the base of Vera Rubin ridge to collect imaging data of outcrops exposed in the vertical faces to investigate the stratigraphic relationship between Vera Rubin ridge and Glen Torridon strata.
3. *Smooth-ridged clay-bearing unit type example:* This waypoint is in the region that exhibits some of the deepest ∼1.9 and ∼2.28 μm spectral absorptions attributed to smectite in lower Mount Sharp, and it is representative of the "smooth" part of the clay-bearing unit. This waypoint is the lowest elevation that *Curiosity* encountered in Glen Torridon, and therefore was identified as a potential drill location to capture the mineralogy of the smooth clay-bearing unit and the lowest stratigraphy in the trough. Additionally, selecting Waypoint 3 as the first drill in this area would enable a drill cadence of ∼every 25 m in elevation within Glen Torridon.
4. *Ridges:* The NE/SW trending ridges located within Glen Torridon were hypothesized to be either depositional features, such as lithified eolian sand dunes, or erosional features, such as periodic bedrock ridges.
5. *Vertical outcrops:* This area includes a set of scarps that form a small valley (informally called the "Visionarium") where vertical outcrops a few meters tall were present on multiple sides of the anticipated rover traverse, enabling 3D reconstructions of the stratigraphy and sedimentary structures.
6. *Fractured clay-bearing unit type example:* This waypoint is representative of the "fractured" part of the clay-bearing unit and is roughly 25 m in elevation above Waypoint 3, which designated it as a potential drill site.
7. *The buttes:* The traverse skirts three buttes to observe the stratigraphy of the area in three dimensions and assess the capping units for comparison to Greenheugh pediment.
8. *Greenheugh pediment:* The capping unit overlying the Greenheugh pediment surface is hypothesized to unconformably overlie the Mount Sharp group and forms a continuation of the Base(al) Siccar Point group unconformity, as observed at Emerson plateau, Naukluft plateau, and the Murray Buttes (Banham et al., 2018, 2021; Bedford et al., 2020). Access to the capping unit was dependent on the rover's ability to climb the ∼10 m tall escarpments, and the attempts would also provide access to exposed strata below the pediment unconformity.
9. *Fractured intermediate unit type example:* This waypoint is representative of the fractured intermediate unit within Glen Torridon and is roughly 25 m in elevation above Waypoint 6, which designated it as a potential drill site.
10. *The Mg sulfate-bearing unit:* The MSL team prioritized exploration of the sulfate-bearing unit for the next portion of the mission after the conclusion of the Glen Torridon campaign. The safest route to approach the sulfate-bearing unit required driving to the east, around a large sand deposit called the Sands of Forvie. The Glen Torridon campaign concluded upon reaching this area.

A preliminary traverse was defined based on the above waypoints. This traverse ended up as a "z" shape across the terrain, starting ENE along the Vera Rubin ridge scarp, then traversing SSW across Glen Torridon to the buttes and Greenheugh pediment scarp (Figure 5). After briefly ascending the scarp to sample the pediment, the rover descended again and drove east around the extensive Sands of Forvie ripple field, to begin the next phase of

Table 2
Summary of Activities Throughout the Glen Torridon Campaign

Traverse segment	Mars sol range	Description
Along the VRR scarp (WAYPOINTS 1–3)	2300–2309	Drive off VRR into GT; investigate first ridge feature
	2309–2361	Drive through rubbly unit along VRR scarp, with stops for investigating sporadic occurrences of coherent bedrock
	2361–2407	Kilmarie and Aberlady 1 and 2 drill holes in the Jura member
	2407–2416	Sand investigation and search for drillable bedrock of high-K compositional endmember
	2416–2429	Woodland Bay outcrop investigation
Ridge features through Glen Etive (WAYPOINTS 4–6)	2429–2447	Ridge feature investigation
	2447–2477	Investigation of Visionarium, including the Harlaw area
	2477–2555	Glen Etive and Glen Etive 2 drill holes in the Knockfarril Hill member
	2509–2522	Solar conjuction
	2522–2555	Finish Glen Etive drill activities
The Buttes (WAYPOINT 7)	2555–2568	Leave Glen Etive and drive toward the buttes
	2568–2590	Investigation of central butte
	2590–2654	Approach and investigation of Western butte
	2654–2664	Approach and investigation of Tower butte
	2664–2691	Hutton drill hole in the "Hutton interval" of the Glasgow member
Greenheugh pediment (WAYPOINT 8)	2691–2702	Drive up onto the pediment
	2702–2729	Edinburgh drill hole in the Stimson formation
	2729–2734	Drive off the pediment
Along the pediment scarp (WAYPOINT 9)	2734–2747	Finish Tower butte investigation
	2747–2780	Glasgow drill hole in the Glasgow member
	2780–2795	Drive across Glasgow member along pediment scarp
	2795–2802	Bloodstone Hill investigation
Deviation to Mary Anning and Groken	2802–2829	Drive downslope to obtain a drill in the Knockfarril Hill member
	2829–2904	Mary Anning and Mary Anning 3 drill holes into the Knockfarril Hill member
	2904–2923	Groken drill hole into a Mg-rich area in the Knockfarril Hill member
Toward the sulfate-bearing unit (WAYPOINT 10)	2923–2951	Investigation of topographic benches
	2951–2967	Drive across the Glasgow member
	2967–3000	Sands of Forvie sand sheet investigation
	3000–3052	Drive across the Glasgow member, approaching the sulfate-bearing unit
	3052–3072	Nontron drill hole in the Glasgow member

its mission accessing and exploring the sulfate-bearing unit. Additional stops and route deviations are described in the detailed description of the traverse below.

4.2. Description of Traverse Segments and Findings

A breakdown of the campaign traverse is included in Table 2 and key results are described in this section.

4.2.1. Along the Vera Rubin Ridge Scarp (Sols 2300–2416; Waypoints 1–3)

The first leg of the Glen Torridon traverse focused on initial characterization of the Glen Torridon surface materials while also carrying out remote sensing of stratigraphy exposed along the adjacent Vera Rubin ridge scarp. *Curiosity* descended from Vera Rubin ridge along a feature nicknamed the "Spur" (Figure 6) that acted as a

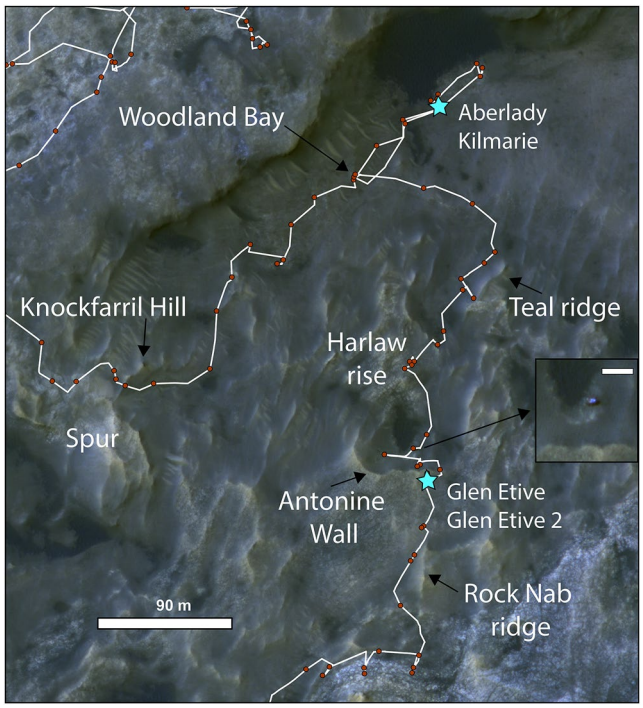

Figure 6. Detailed view of the traverse from the Vera Rubin ridge descent to the start of the butte investigation. Background: HiRISE image ESP_060840_1750. The white line is the rover traverse path and the brown circles are stops along the traverse. The blue stars are drill locations. Inset shows a HiRISE image (ESP_037117_1755) of Curiosity investigating a small impact crater near Antonine Wall (scalebar is 10 m).

ramp with shallow slopes for safe driving (Waypoint 1). Next, the rover drove over and imaged a ridge that was capped with a block exhibiting crossbedding, called Knockfarril Hill (Figures 6 and 7). This outcrop was later recognized as the first occurrence of cross-bedded sandstones that in part define the Knockfarril Hill member (Fedo et al., 2022).

Curiosity drove ~340 m ENE along the base of Vera Rubin ridge (Waypoint 2) but found relatively little bedrock exposed along the ridge's steep margin compared to abundant talus, coarsely surfaced megaripples, and deposits of dark sand banked against the lower flanks of the ridge (Figure 7; Sullivan et al., 2022). The heavily eroded terrain explains the smooth character of the region in HiRISE images, as surface features less than roughly 1 m across are unresolved even at 25 cm per pixel (McEwen et al., 2007). The trough floor along this traverse segment is dominated by regolith, with distinctive pebble- to cobble-sized mudstone clasts (Khan et al., 2022). Bedrock, sometimes thinly mantled with regolith, is exposed in systems of polygons each typically tens of cm across and generally exhibiting little surface relief, divided from each other by narrow lanes of regolith that in many cases demonstrates evidence for recent deformation and activity (Hallet et al., 2022). The exposures of coherent bedrock are both finely laminated mudstone and examples of cross-bedded sandstone (Caravaca et al., 2022), and the rocks in this portion of the traverse were classified as part of the Jura stratigraphic member (Figure 8).

Both the APXS and ChemCam instruments made compositional measurements at regular intervals along the first leg of the traverse, documenting bedrock as well as clasts and regolith. Both instruments documented that the bulk elemental composition of Glen Torridon is consistent with other strata in the Mount Sharp group (Dehouck et al., 2022; O'Connell-Cooper et al., 2022), but noted two distinct chemical endmember populations that generally correspond to two different types of outcrop expressions. The pebble- to cobble-sized mudstone rubble that covers much of the landscape are generally enriched in K_2O (>1.5 wt%) and SiO_2 (>55 wt%) compared to the larger, coarser-grained coherent blocks that are relatively enriched in MgO (>6 wt %) (Caravaca et al., 2022; Dehouck et al., 2022; O'Connell-Cooper et al., 2022). ChemCam

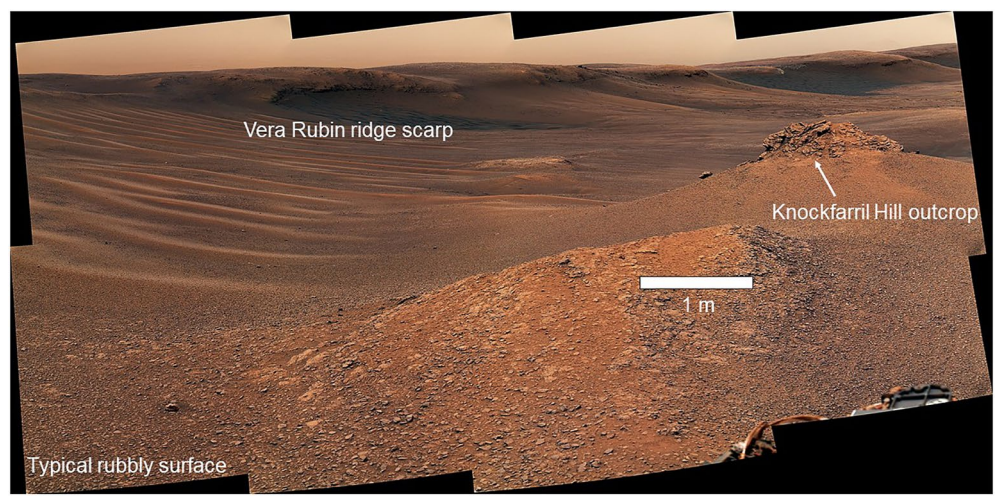

Figure 7. Mastcam mosaic (2309ML012330; NASA/JPL-Caltech/MSSS) acquired shortly after entering Glen Torridon. The mosaic shows the southern scarp of Vera Rubin ridge, the crossbedded Knockfarril Hill outcrop, and the typical heavily ("rubbly") eroded surface texture that gives the clay-bearing unit's characteristic smooth texture in HiRISE images. Light-toned mega ripples are visible on the left side of the image.

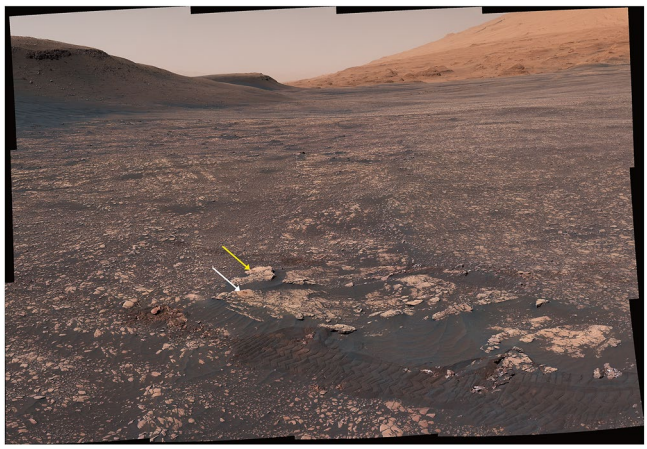

Figure 8. Context Mastcam view of the Waypoint 3 area, looking East along Vera Rubin ridge on the left and toward Mt Sharp on the right. The white and yellow arrows points to the Aberlady and Kilmarie drill holes, respectively. The rover tracks in the foreground are ~40 cm wide. This region is representative of the highly eroded terrain characteristic of lower Glen Torridon, which made locating blocks of sufficient size to drill challenging. Refer to Figure 6 for the orbital context (2411ML012780; NASA/JPL-Caltech/MSSS).

also documented targets with elevated copper content within Glen Torridon, primarily within the coherent blocks that outcrop in the Jura member and only in one spatially constrained area in the Knockfarril Hill member (Goetz et al., 2022). The DAN instrument also conducted regular active neutron source activities to characterize the Water Equivalent Hydrogen in the shallow surface and found that values increased in Glen Torridon compared to Vera Rubin ridge (Czarnecki et al., 2022). This observation of increased hydration correlates with observations from CRISM, which detects relatively deep 3 μm absorption bands caused by H_2O molecular vibrations in the northernmost regions of Glen Torridon along Vera Rubin ridge (He et al., 2022).

By the time Curiosity arrived in the Waypoint 3 area, the terrain in lower Glen Torridon had been sufficiently characterized to be able to choose a representative target for the CheMin and SAM instruments. The first drill target, called Aberlady (Figure 8), was determined to be in the high Mg/low K endmember group (Dehouck et al., 2022; O'Connell-Cooper et al., 2022). The Aberlady block fractured due to the drilling disturbance and the amount of sample collected was insufficient to conduct all the desired experiments. Therefore, a second drill location was selected on an adjacent block less than a meter away, called Kilmarie. MAHLI images of drill holes are shown in Figure 9. X-Ray diffraction results found that the samples contained abundant phyllosilicates (primarily dioctahedral smectites), feldspar, plagioclase, and calcium sulfates, with only a small amount of hematite (Thorpe et al., 2022); mineralogically, these samples are comparable with the rest of the Mount Sharp group, and consistent with predictions from CRISM reflectance measurements (He et al., 2022). Two new minor phases were identified by the CheMin X-ray diffraction instrument for the first time in the Kilmarie drill sample: Fe-carbonate and a mineral phase that has a novel peak at 9.2 Å whose identity remains debated (Bristow et al., 2021; Thorpe et al., 2022). The SAM instrument analyzed the Kilmarie sample for organic molecules, and found chlorohydrocarbons and nitrogen-bearing organics, which are known thermal decomposition products of the SAM wet chemistry reagent(s) and chemical reactions with chlorine-bearing minerals such as chlorides (Millan et al., 2022). The lack of organics in the rocks of Kilmarie may be explained by its proximity with the diagenetically altered VRR (Millan et al., 2022).

After the Aberlady and Kilmarie drill campaign was completed, the rover measured modern sand ripple structure and composition in a nearby active dark sand deposit to assess the modern aeolian environment (Sullivan et al., 2022; Weitz et al., 2022). Several sols were then dedicated to searching for a representative high-K outcrop that was large enough to drill, as the rover requires a flat surface at least 10 cm across on which to place the drill turret. However, given that the high-K endmember group is also characteristically comprised of pebble and cobble-sized clasts, a drillable rock was not identified and the Glen Torridon campaign continued.

Along the initial traverse to Waypoint 3, a facies with distinctive alternating thin and thick laminae was identified at several points along the base of the Vera Rubin ridge scarp (Fedo et al., 2022). After completing the drill campaign and sand investigation at Waypoint 3, the rover returned to a particularly well-exposed example of this facies (called the Flodigarry facies; Fedo et al., 2022) at the target Woodland Bay (Figure 10). Once there, the rover collected detailed compositional and imaging measurements to help constrain the petrogenesis of the pebble-forming protolith, the compositional endmembers, and the stratigraphic relationship between Glen Torridon and Vera Rubin ridge (Caravaca et al., 2022; Dehouck et al., 2022; Fedo et al., 2022; O'Connell-Cooper et al., 2022). Data from the Woodland Bay outcrop was used to interpret that the northern edge of Glen Torridon is stratigraphically equivalent to Vera Rubin ridge because this thinly and thickly laminated facies appears at equivalent elevations in Glen Torridon and on Vera Rubin ridge (Figure 3; Fedo et al., 2022). Therefore, despite the geomorphic distinction between the Vera Rubin ridge and the Glen Torridon trough, strata at the top of the ridge and the bottom of the trough are both interpreted to be part of the Jura stratigraphic member of the Murray formation.

4.2.2. Linear Ridge Features Through Glen Etive (Sols 2416–2568; Waypoints 4–6)

After examining the Woodland Bay target area, the rover headed SSW across the trough floor, gradually upslope (Figure 6). The next waypoint investigated one of the low, NE-SW trending linear ridges that occur widely throughout Glen Torridon, called Teal ridge (Waypoint 4). Comparative imaging and compositional observations

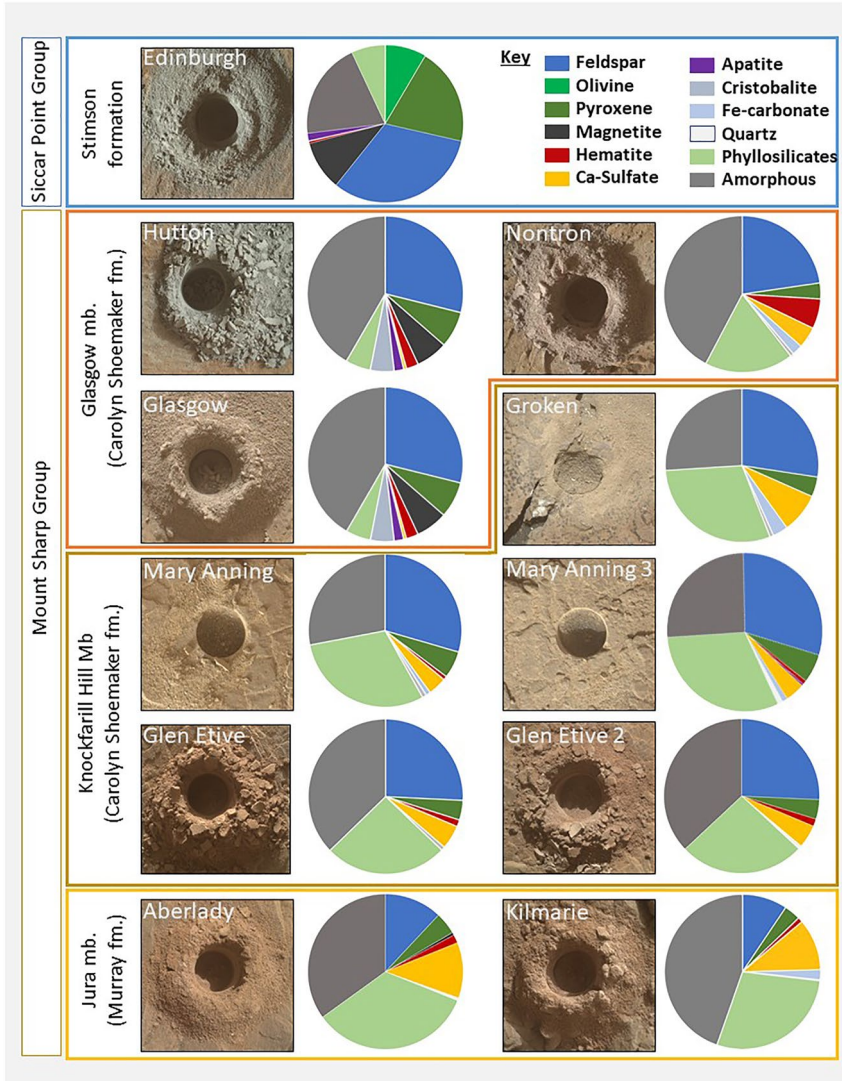

Figure 9. Mars Hand Lens Imager (MAHLI) image and CheMin bulk mineralogy of drilled samples withing the Glen Torridon region. The drill hole is ~1.6 cm in diameter. MAHLI Images used—Aberlady: 2378MH0007740010900199C00; Kilmarie: 2404MH0007740010900288C00; Glen Etive: 2524MH0007740010903140C00; Glen Etive 2: 2550MH0007740010903254C00; Glasgow: 2773MH0004240011002826C00; Mary Anning: 2851MH0001970011003289C00; Mary Anning 3: 2890MH0004240011003450C00; Groken: 2920MH0004240011003512C00; Hutton: 2684MH0007740011001668C00; Nontron: 3068MH0007740011101168C00; and Edinburgh: 2724MH0007740011002434C00.

were aquired at both the base and crest of the ridge. Ridge slopes are covered with loose sand and clasts, but the southern end of the crest is capped by coherent bedrock that is similar to the cross-stratified Knockfarril Hill outcrop (Figure 11; Fedo et al., 2022; Stack et al., 2022). The Teal ridge investigation, together with observations of other related features, found that these low ridges incorporate contiguous local bedrock stratigraphy of the Mount Sharp group, consistent with their interpretation as Periodic Bedrock Ridges eroded by salting sand (cf., Montgomery et al., 2012), rather than as unconformable lithified aeolian bedforms (Stack et al., 2022).

As predicted based on HiRISE image analysis, the Visionarium (Waypoint 5) provided multiple opportunities to investigate bedrock outcrops that create a natural set of varied orientations, across almost 270° in azimuth where bedding geometries can be deduced. Arrival in this region marked a significant change in the overall terrain, as the heavily eroded, clast-dominated landscape gave way to cross-stratified sandstones that outcropped frequently (Caravaca et al., 2022) at the first stop in this area, called Harlaw rise (Figures 6 and 11). Interfingering beds

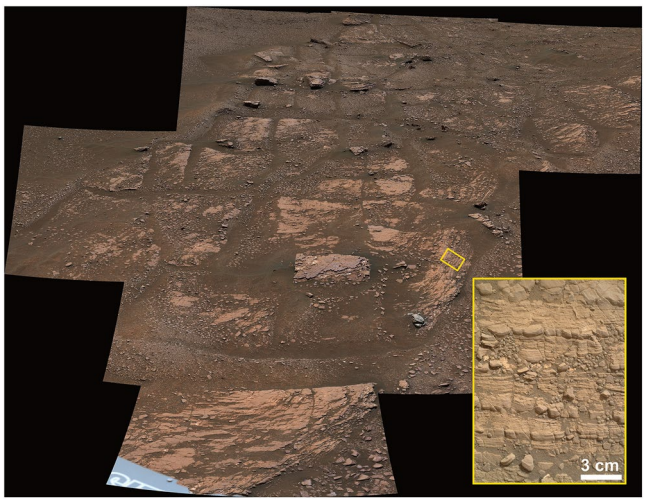

Figure 10. Mastcam mosaic (2359ML12506; NASA/JPL-Caltech/MSSS) of the Woodland Bay target area, which demonstrates the typical bedrock outcrop appearance throughout lower Glen Torridon, as well as the polygonal troughs that form around blocks. Inset (~10 × 15 cm) showcases a Mars Hand Lens Imager (MAHLI) close-up of the Morningside target, an example of the thin-thick laminations in mudstone bedrock that helped classify these rocks as stratigraphically part of the Jura member (MAHLI image; 2424MH0001900010900914C00). Refer to Figure 6 for orbital context.

of this sandstone and the fine-grained lacustrine mudstones that are typical of the Murray formation represent a progressive transition in this area (Caravaca et al., 2022). The change in the predominant lithology that started here contributed to the decision to define the Knockfarril Hill member as the base of the new Carolyn Shoemaker formation, with cross-stratified sandstones marking its base (Fedo et al., 2022).

The final stop in the Visionarium was Antonine Wall (Figure 12), a ~2.5 m tall scarp feature with well-exposed layering. At this outcrop *Curiosity* obtained compositional data (bulk elemental abundances did not significantly vary from previous regions (Dehouck et al., 2022; O'Connell-Cooper et al., 2022)) and Mastcam mosaics, then drove around and on top of the outcrop to drill (Figure 13). This site in the Knockfarril Hill member represented a unique observational opportunity due to the detailed observations obtained of the outcrop below the drill location at Antonine Wall, enabling better 3-dimensional contextualization. Two drill holes (Glen Etive, Glen Etive 2) were needed to obtain enough sample material for the CheMin and SAM experiments. The Glen Etive drill hole contains the highest abundance of clay minerals thus far analyzed within a drill sample in Gale crater (34 wt. %; Bristow et al., 2021; Thorpe et al., 2022). After finishing drill activities at Glen Etive, the rover stopped briefly to wheel-scuff and analyze a large, coarsely surfaced megaripple, considered similar to features along the base of Vera Rubin ridge that could not be approached closely (Sullivan et al., 2022; Weitz et al., 2022). *Curiosity* then continued upslope southward to document a ridge ("Rock Nab") for comparison with other periodic bedrock ridges.

4.2.3. The Buttes and the Glasgow Member (Sols 2568–2691; 2735–2780, Waypoint 7)

Curiosity investigated three buttes in Glen Torridon: Central butte, Western butte, and Tower butte (Figures 14 and 15). Preserved cap rock on the top of each butte is progressively less with distance from the current Green-

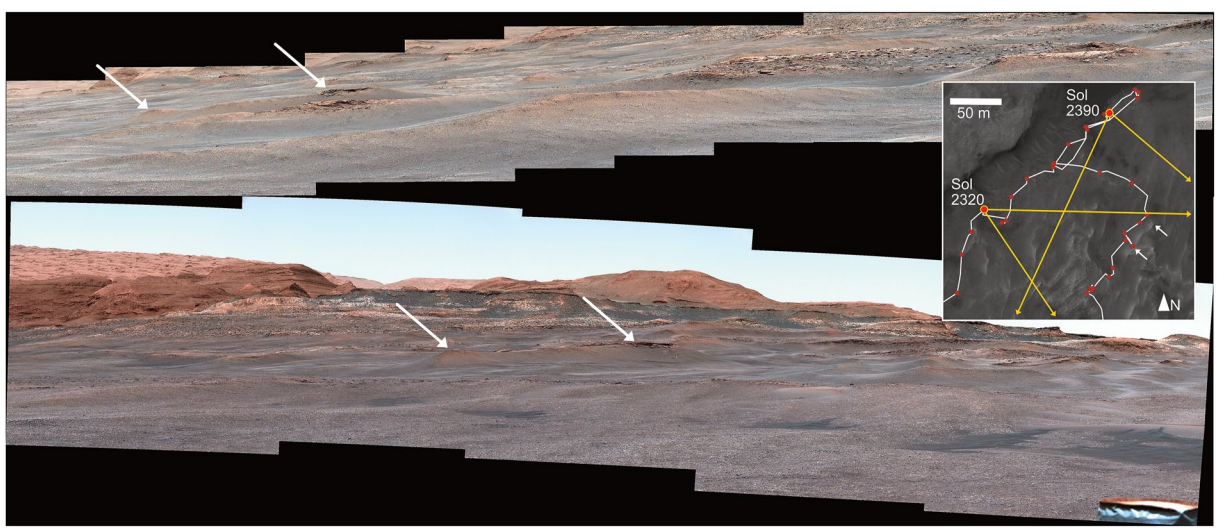

Figure 11. Linear ridges that trend NE-SW are especially pronounced in the northern region of Glen Torridon and are capped by Knockfarril Hill member crossbedded sandstones when they extend farther south. Both images here show some of the same landscape features from different viewing angles. Upper image: Mastcam mosaic acquired on Sol 2320 looking E-SE from the rover's position across several ridges, some of which have cross-bedded sandstone caps on their southern ends (2320ML12396, NASA/JPL-Caltech/MSSS). Lower image: Mastcam mosaic acquired on sol 2390 looking south from the rover's position toward the linear ridges, with the Greenheugh pediment scarp and Mount Sharp in the background (2390ML12686, NASA/JPL/MSSS). Inset: HiRISE context of Curiosity's traverse in white, indicating the view angles of both mosaics. In all images, white arrows point to the northern and southern ends of Teal Ridge, which was investigated in-situ by Curiosity. Arrow points are ~30 m apart along the crest of Teal ridge.

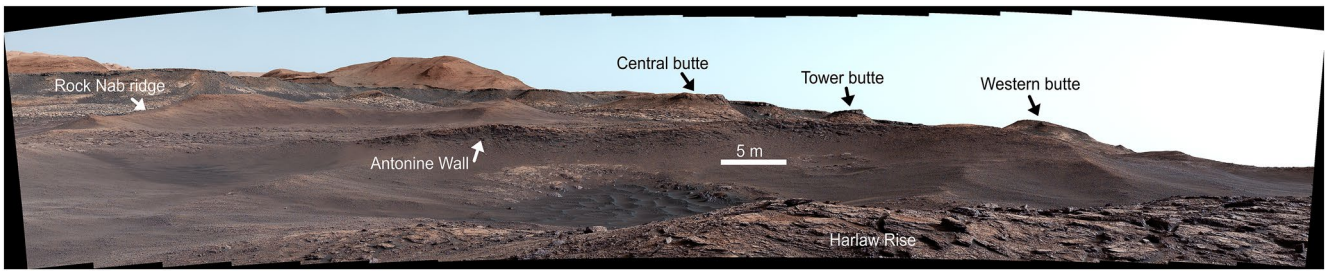

Figure 12. Mastcam mosaic (2458ML13044, NASA/JPL-Caltech/MSSS) acquired from Harlaw rise (in foreground) on sol 2458 looking south toward Antonine Wall while Curiosity was characterizing the exposed stratigraphy around waypoint 5. Visible in the background are Rock Nab ridge, several buttes, and the pediment scarp, all eventually investigated in situ. Refer to Figure 6 for orbital context.

heugh pediment edge. Investigating the buttes from multiple angles allowed for three-dimensional views of the stratigraphy and access to an addition ∼10 m of vertical outcrop expression.

The rover first explored Central butte and made two short transects up the side of the butte through well-exposed stratification, documenting sedimentary textures and compositional variation. The contact between the Knockfarril Hill member and the overlying Glasgow member is exposed in the base of Central butte; the contact is placed at the top of the last sandstone bed before a return to finely laminated sediments (Fedo et al., 2022). *Curiosity* next visited Western butte, which is higher in elevation than Central butte and consists of rocks in the Glasgow member. Exploration of Western butte revealed abundant diagenetic features, such as nodules (Gasda et al., 2022). The bedrock exposed at Western butte is typically gray in color and has a chemical composition that deviates from the rest of Glen Torridon (Dehouck et al., 2022). *Curiosity* drove up the side of Western butte and reached a point near the top of the butte before the terrain became too steep to proceed. Float rocks inferred to be from the capping deposit on Western butte were sandstones that lack crossbedding, but otherwise resemble Stimson sandstones, and had anomalous composition compared to the expected Stimson formation (Thompson et al., 2022).

Finally, Tower butte is located very close to the edge of Greenheugh pediment (Figures 14 and 15) and provided an opportunity to investigate the relationship between the buttes and the pediment, as well as the contact between Mount Sharp group sediments and the overlying Siccar Point group capping unit (Figure 16). The Glasgow bedrock below the pediment cap in Tower butte is light-toned and rich in nodules and veins (Figure 17). As *Curiosity* approached the pediment, rocks broken by the rover driving over them revealed a bright gray tone,

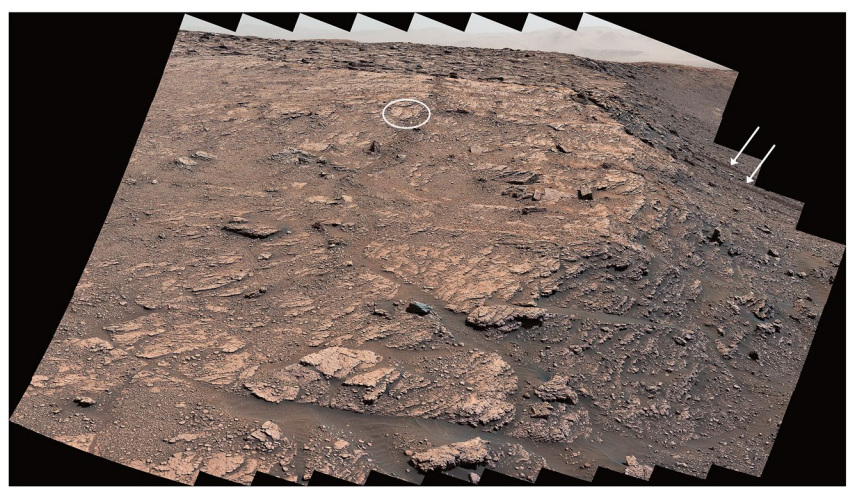

Figure 13. Mastcam mosaic (2480ML13164, NASA/JPL-Caltech/MSSS) obtained on sol 2480 looking west, as the rover drove out of the Visionarium to approach the Glen Etive drill site. The white circle indicates the block from which the Glen Etive samples would be collected, and the white arrows points to the rover tracks from where Curiosity approached the target Antonine Wall to investigate the 3-dimensional structure of this outcrop. The wheel tracks are 40 cm wide and spaced approximately 3 m apart. Refer to Figure 6 for orbital context.

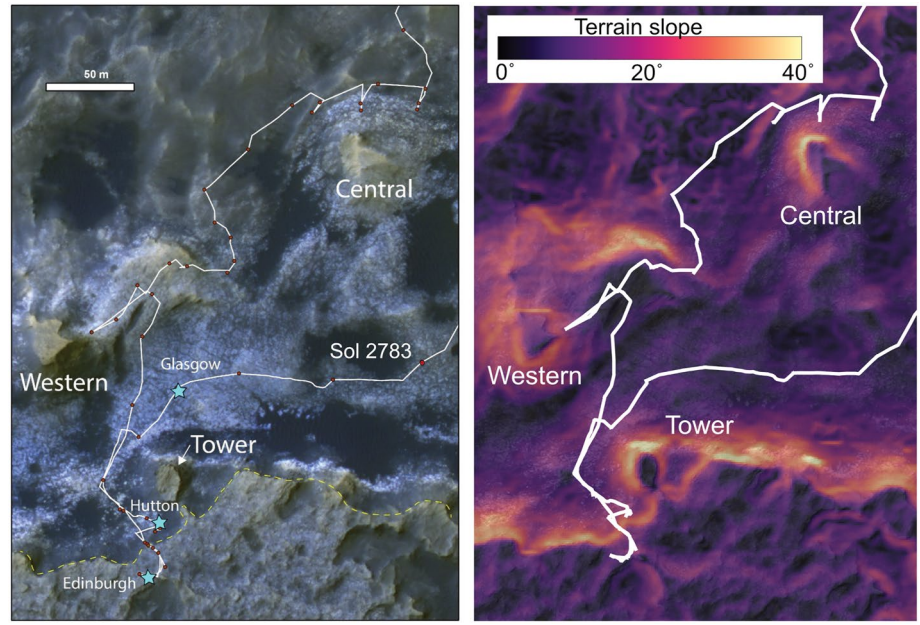

Figure 14. Left: Detailed view of the traverse through the buttes and the pediment campaign. Background: HiRISE image ESP_060840_1750. The white line is the rover traverse path and the brown circles are stops along the traverse. The blue stars are drill locations. Right: Map of terrain slopes, derived from the HiRISE DEMs, showing the topography of the buttes and pediment scarp. Curiosity reached a maximum rover tilt of 32° while driving to the Edinburgh drill site. The text "sol 2783" marks where the mosaic in Figure 17 was obtained.

especially close to the pediment capping unit—this zone of anomalous color is called the Hutton interval (Figure 16). *Curiosity* was able to drive onto a topographic bench near Tower butte to investigate this section of color variations. The capping rocks on top of Tower butte were similar to those on Greenheugh pediment itself (Section 4.2.4).

To capture differences in mineralogy and/or redox state between materials of different colors and to test the hypothesis that the color variations are due to diagenesis, the rover collected two drill samples within the Glasgow member. The Glasgow drill sampled a representative Glasgow member facies that was the typical gray in color, and the Hutton drill sampled the anomalously light-toned Hutton interval on the bench feature near Tower butte (Figures 16 and 17). For comparison, the Aberlady, Kilmarie, and Glen Etive drills were obtained in relatively red rocks (Figure 9; Sections 4.2.1 and 4.2.2) from within the Jura and Knockfarril Hill members.

The Hutton drill sample contains cristobalite, opal CT, and magnetite in higher abundances than elsewhere in Glen Torridon (Thorpe et al., 2022). There are also fewer clay-minerals in this interval (~6 wt. %; Thorpe et al., 2022) and Mastcam multispectral data suggest a lack of Fe^{3+}-bearing minerals (Rudolph et al., 2022). This area is enriched in the mobile elements Na, Ca, and Mg and depleted in S (Thompson et al., 2022), and displays a lower Chemical Index of Alteration (CIA; Dehouck et al., 2022). The Hutton interval contains abundant diagenetic features such as nodules, light and dark veins, and hollow circular features (Rudolph et al., 2022) that exhibit an array of geochemical compositions, particularly enrichments in Mn, Mg, Fe, and K (Gasda et al., 2022; Thompson et al., 2022).

The SAM pyrolysis-GCMS analyses of Glen Etive, Glasgow, and Hutton, led to the detection of the greatest diversity abundance and diversity of sulfur-bearing organic molecules yet detected in Gale crater (Millan et al., 2022). Some of these sulfur-bearing organics such as dimethylsulfide and the thiophene derivatives were previously detected at Pahrump Hills in Gale crater (Eigenbrode et al., 2018) while the presence of other S-bearing molecules such as dithiapentane were only suspected in previous analyses. New S-organics were also highlighted in these specific samples and include the aliphatic propanethiol and the dithiolane and trithiane aromatic compounds (Millan et al., 2022). The detection of these S-organics extracted at high pyrolysis temperature (>600°C), only in these specific samples and combined with the fact that they were not detected in SAM-like laboratory experi-

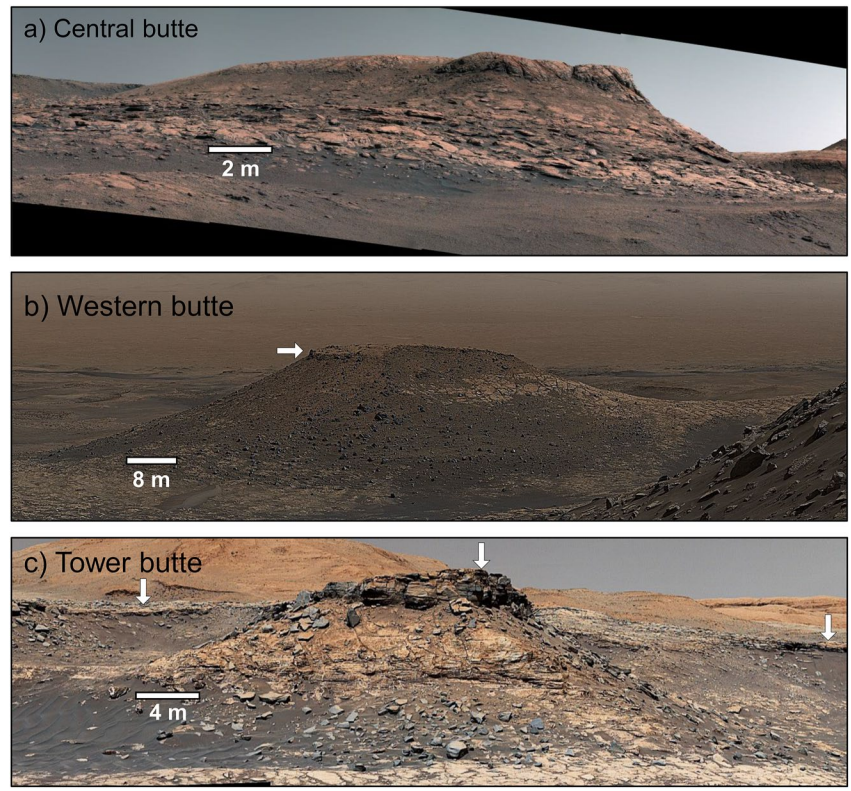

Figure 15. Mastcam mosaics of the buttes. The white arrows point to the Stimson formation that caps the pediment. Note that there is no capping unit at Central butte. (a) Central butte (2568ML013483; NASA/JPL-Caltech/MSSS), (b) Western butte (2671ML014006; NASA/JPL-Caltech/MSSS), and (c) Tower butte (2628ML013757; NASA/JPL-Caltech/MSSS).

ments of analogs indicate that they are likely indigenous to the sample and that they are likely fragments of recalcitrant organic matter preserved within the samples and that decomposed during pyrolysis (Millan et al., 2022).

4.2.4. The Greenheugh Pediment (Sols 2691–2734; Waypoint 8)

Determining the origin of the rocks that form the pediment-capping unit and investigating the contact between the capping unit and the underlying Hutton interval was a high priority investigation, contingent on whether-or-not the rover could physically access the targets due to the steep slope of the escarpment. After a challenging drive (where the rover achieved a record tilt of 32.0°), *Curiosity* safely reached the top of the pediment scarp near Tower butte (Figure 14). The ascent included stops to investigate the contact between the Mount Sharp group and the overlying capping unit.

Observations made during the ascent and traverse over the pediment top revealed blocky, blue-gray colored weathering resistant outcrops composed of medium-grained crossbedded sandstones (Figures 16 and 18). Based on their stratigraphic position, sedimentary texture and architecture, the pediment capping unit is interpreted to be part of the Stimson formation that belongs to the Siccar Point group (Banham et al., 2022). Mudstone intraclasts with a similar appearance to the underlying Carolyn Shoemaker formation occur at the contact, demonstrating sedimentary recycling during deposition (Banham et al., 2022). ChemCam analyses of these Stimson unconformity targets confirmed the recycling of Carolyn Shoemaker grains with the Stimson sand dunes (Bedford et al., 2022).

The capping sandstones have been subdivided into the basal Gleann Beag interval, characterized by platy weathering, and the Ladder and Edinburgh intervals, characterized by their blockier, more massive appearance (Banham et al., 2022). At the pediment ascent location, evidence for changes of dune morphology and dune migration direction were identified and they were interpreted to be wrought by fluctuations in wind strength and direction at seasonal through to millennial time scales (Banham et al., 2022). After investigating sedimentary structures and grain sizes, the Edinburgh drill sample was acquired in the Stimson formation and then *Curiosity*

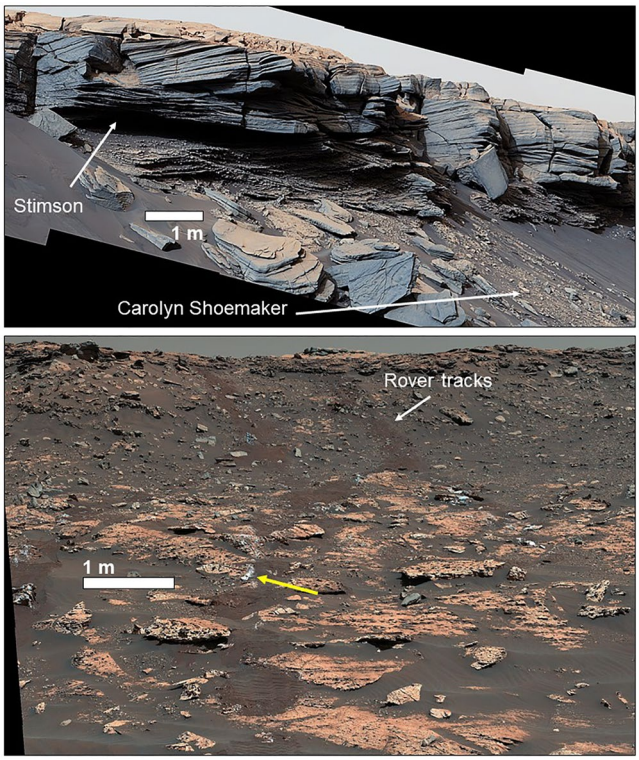

Figure 16. Mastcam mosaics of the pediment and pediment scarp. (a) The contact between the Stimson formation sandstones and the underlying Carolyn Shoemaker formation mudstones (shown by white arrows). The contact and the Carolyn Shoemaker formation are covered by sand and debris (2685MR014053; NASA/JPL-Caltech/MSSS). (b) The location where Curiosity ascended a 32° slope to reach the top of the pediment. Rover tracks (from both the ascent and descent) are visible (white arrow). The strata beneath the capping Stimson formation are part of the Hutton interval, and the characteristic light-toned color of this interval is visible where the rover tracks either crushed or broke open rocks to reveal fresh surfaces (yellow arrow) (2737MR014348; NASA/JPL-Caltech/MSSS).

descended the pediment scarp the same way it came up. CheMin results from the Edinburgh drill sample are consistent with the pediment capping unit being enriched in igneous minerals (e.g., plagioclase, pyroxene, and olivine) and magnetite while low in clay minerals (Figure 9). Together, the mineralogy of Edinburgh suggests the pediment capping unit experienced fundamentally different conditions during sedimentation than during diagenesis (e.g., Thorpe et al., 2022).

Analysis using ChemCam indicated that this part of the Stimson is within the geochemical range of the Stimson formation investigated by ChemCam at the Emerson and Naukluft plateaus. However, the Greenheugh pediment capping unit has a subtle, but statistically significant higher abundance of MgO, and lower abundances of SiO_2 compared to the Stimson formation at the Emerson and Naukluft plateaus, suggestive of a more mafic sediment source (Bedford et al., 2022). Geochemical data acquired by APXS indicated a distinct composition for the Ladder and Edinburgh interval sandstones (>K_2O, Na_2O, MnO, FeO, and Cr_2O_3) versus the Gleann Beag sandstones exposed in the lower section of the pediment caprock, and typical Stimson sandstones as measured at locations lower on Mount Sharp (Thompson et al., 2022). The geochemical differences identified by ChemCam and APXS between the Ladder and Edinburgh interval and the Emerson/Naukluft Stimson sandstones are also reflected in the mineralogy determined by CheMin (Thompson et al., 2022). The Edinburgh drill sample contains more abundant sanidine than detected in previous Stimson drilled samples, as well as 8.4% olivine and 7% smectite (phases previously undetected in Stimson samples) (Thorpe et al., 2022). This could reflect input of alkaline detritus to the pediment Stimson sandstones (Thompson et al., 2022), as has also been suggested for other previously encountered K-rich sandstones (Thompson et al., 2016).

The Stimson formation at the Greenheugh pediment lacks evidence of significant aqueous alteration well above the unconformity, such as extensive calcium-sulfate mineral veins or fracture associated halos, implying that there was less groundwater availability at this site compared to those previously characterized (Bedford et al., 2022). Aside from the sandstone cement, diagenetic fluids were largely restricted to an interval just above the unconformity where concretions that are geochemically similar to the non-concretionary bedrock occur (Bedford et al., 2022). Such concretions also occur in other localities at the base of the Stimson formation, supporting that they formed through the preferential cementation of the Stimson formation at the base (Banham et al., 2018; Bedford et al., 2022). However, the secondary mineralogy of the Greenheugh pediment contains negligible hematite and has poorly formed phyllosilicates, suggesting that the Stimson formation at this locality was cemented with a different fluid to that which cemented the Stimson formation at the Emerson and Naukluft plateaus (Bedford et al., 2022; Rampe, Blake, et al., 2020).

Figure 17. Mastcam mosaic (2783ML14571, NASA/JPL-Caltech/MSSS) looking toward the northeast from the rover position on sol 2783 over typical exposures of Glasgow member bedrock. The southern scarp of Vera Rubin ridge is visible in the background.

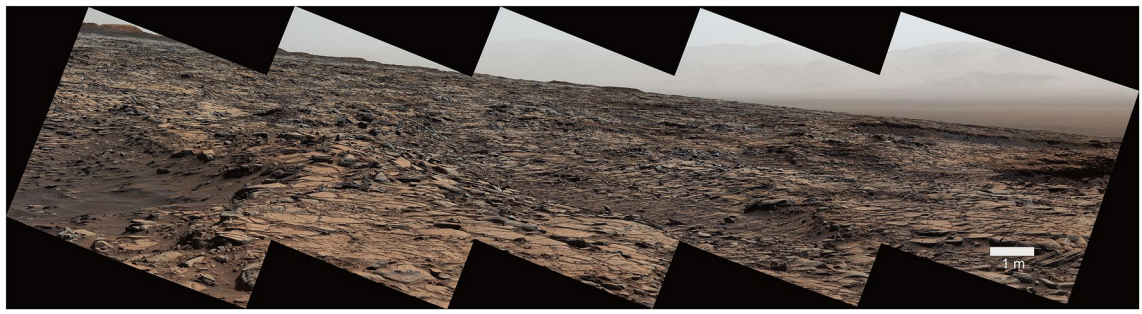

Figure 18. Mastcam mosaic (2698ML14123, NASA/JPL-Caltech/MSSS) acquired on sol 2698 near the Edinburgh drill location, looking west across the Greenheugh pediment cap. The cliff edge is visible on the right side of the image, and Gale crater's rim is faintly visible in the background.

4.2.5. Transit Along the Base of the Pediment Scarp (Sols 2780–2802; Waypoint 9)

The primary goal of this section of the rover traverse (Figure 19) was to characterize the Glasgow member and document stratigraphy exposed in the pediment scarp. The final stop on this traverse leg was Bloodstone Hill (Figure 20), a prominent light-toned butte visible from *Curiosity*'s landing site (Johnson et al., 2016) at the eastern-most extent of the pediment edge that parallels Vera Rubin ridge. The butte lacks continuous Stimson capping rock. Instead, isolated Stimson boulders are scattered across the top and slopes of the butte. The Glasgow member bedding is finely laminated but coarse nodules and frequent veins disrupt the exposure.

4.2.6. Deviation to Mary Anning and Groken (Sols 2802–2923)

At this point in the campaign, the rover had traversed nearly 3 km through Glen Torridon strata, collected seven drill samples at five different sites, and the team had established a baseline understanding of the stratigraphy, composition, and depositional history of the region. With this information, the team selected a location (Fedo et al., 2022) for the high priority but resource intensive SAM wet chemistry experiments designed to detect and identify complex organic molecules and characterize the habitability of the past environments in Glen Torridon. Based on laboratory experiments, the TMAH in situ experiment was expected to optimally perform with phyllosilicate-rich mineral assemblages, so the rover returned to the Knockfarril Hill member to conduct further drill activities (Figure 19). Directing the rover to an optimal site required using characteristic bedrock exposure, surface topographic expression and inferences about strike and dip to project the location of the contact with the Knockfarill Hill member farther to the east beyond Bloodstone Hill. Based on these predictions, *Curiosity* drove to the target location and confirmed the stratigraphic positioning based on presence of cross-bedded sandstones and elemental compositional measurements. In effect, this was a successful test of the use of a combination of rover and orbital observations to construct accurate lithologic maps.

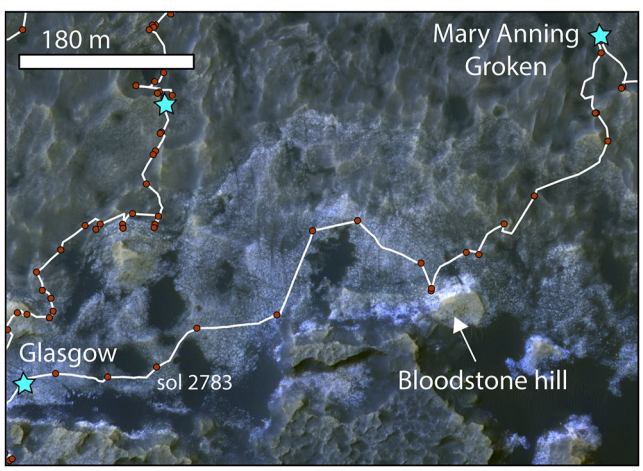

Figure 19. Detailed view of the traverse from the Glasgow drill hole to the Mary Anning drill hole. Background: HiRISE image ESP_060840_1750. The white line is the rover traverse path and the brown circles are stops along the traverse. The blue stars are drill locations. The text "sol 2783" marks where the mosaic in Figure 17 was obtained.

Once clearly within the Knockfarril Hill member, *Curiosity* drilled the Mary Anning target for analysis. Multiple drill holes were needed to obtain sufficient sample quantities for all the desired experiments, so a second drill was acquired close to the original drill site and called Mary Anning 3 (Figure 21; the Mary Anning 2 site was assessed but not selected for drilling). A pyrolysis without derivatization agents (standard SAM-GCMS) was conducted followed by the first time TMAH experiment, and then a MTBSTFA wet chemistry experiment. These SAM-GCMS wet chemistry experiments in Glen Torridon, and especially the TMAH experiment at Mary Anning, liberated a variety of aromatic organic molecules up to two carbon rings (Millan et al., 2022; Williams et al., 2021). Among these aromatic compounds, the nitrogen-bearing molecules detected are likely related to the thermal decomposition of the TMAH reagent, while others are known degradation products of the adsorbent used in the SAM traps (Millan et al., 2022; Williams et al., 2021). However, some of these aromatic compounds including the two methyl-naphthalene isomers, benzothiophene and potentially an alkyl-thiophene, were detected for the first time with SAM. The detection of

Figure 20. Mastcam mosaic (2797ML14656, NASA/JPL-Caltech/MSSS) of the outcrop exposed at Bloodstone Hill.

these aromatics may be related to the presence of macromolecular material as they have been found in several Martian meteorites (McKay, 1996; Mojarro et al., 2021; Steele et al., 2012), and is consistent with the detection of the sulfur-bearing organics (Millan et al., 2022).

While the rover was stationary at Mary Anning and completing the drill activities, *Curiosity* used its remote sensing instrument suite to document the surrounding area. This led to the discovery of MnO-rich nodules with elevated phosphorous that are confined to discrete rock layers, within a few meters of the Mary Anning targets (Gasda et al., 2022). Manganese oxides are only concentrated in highly oxidizing aqueous environments (Lanza et al., 2014), and the identification of an MnO-rich layer of nodules prompted the decision to drill into these unique features at the target Groken (Figure 21). Crystalline Mn or P bearing phases were not detected by CheMin X-ray diffraction analysis of Groken, suggesting either that these elements are part of the X-ray amorphous component, which constitutes ∼27 wt.% of the sample (Thorpe et al., 2022) or the collected sample did not include the nodular material.

4.2.7. Campaign Completion: Heading Toward the Mg Sulfate-Bearing Unit (Sols 2923–3072; Waypoint 10)

The area to the southeast of the Mary Anning drill hole contains a series of topographic benches that *Curiosity* traversed on its way to the Mg sulfate-bearing unit (Figure 22). *Curiosity* collected a series of images and compositional data at the benches to characterize the stratigraphic relationship between the Knockfarril Hill and Glasgow members in this area.

The remainder of this traverse was through the Glasgow member with a brief excursion to the edge of the large Sands of Forvie sand sheet (Figure 23) for compositional and morphological comparisons with other active aeolian dark sand deposits (Christian et al., 2022; He et al., 2022; Sullivan et al., 2022; Weitz et al., 2022). Mission priorities during this traverse segment were to document along-strike variations with the Glasgow member while

Figure 21. Mastcam mosaic (2865ML14954, NASA/JPL-Caltech/MSSS) of the Mary Anning 3 drill site (white arrow). The drill hole is ∼1.6 cm in diameter. The yellow box indicates where MnO-rich nodules were identified by the ChemCam instrument and later drilled; Inset shows Mars Hand Lens Imager image 2906MH0004240011003483C00 of the Groken drill target before the sample was collected. Nodules are visible as the dark spots on the rock.

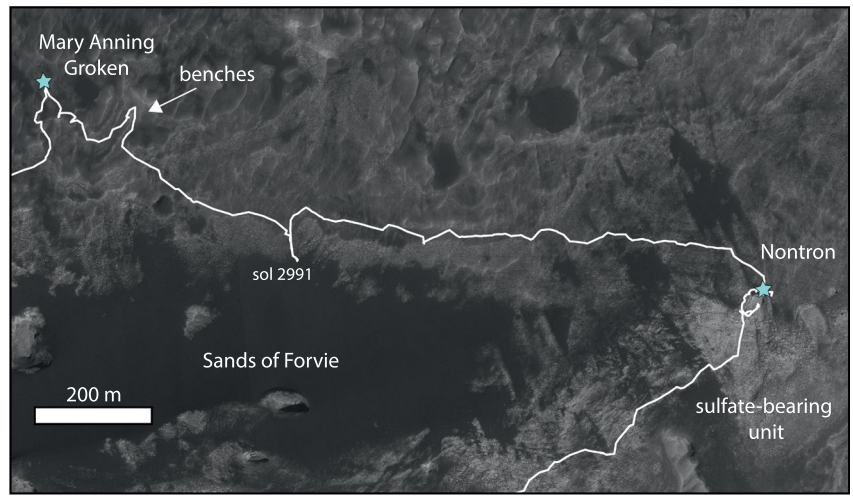

Figure 22. Detailed view of the traverse from the Mary Anning and Groken drill holes past the Sands of Forvie sand sheet to the Nontron drill hole, before the rover began its next mission phase to explore transitional strata to the sulfate-bearing unit. Background: Gale orthophoto mosaic from Calef and Parker (2016). The white line is the rover traverse path and the blue stars are drill locations. The text "sol 2991" marks where the mosaic in Figure 23 was obtained.

driving expeditiously toward the transition to the Mg sulfate-bearing unit, representing the next phase of the MSL mission. As the last activity within the Glen Torridon region, *Curiosity* collected one more drill sample, Nontron, close to the expected transition zone into the Mg sulfate-bearing strata that overlie Glen Torridon to provide comparison as the rover proceeded with its mission (Figure 24). The mineralogy of the Nontron drill sample is similar to other Glasgow member drill samples (Figure 9).

After Glen Torridon, Curiosity's traverse headed into the Mg sulfate-bearing strata and included a stop at another section of the pediment that is further upslope (Figure 2). Preliminary results have shown that most of the sedimentary structures in the strata directly above Glen Torridon have been overprinted by diagenesis. The amount of clay minerals in drill samples decreased as the rover drove further from Glen Torridon, and CheMin has thus far detected no signatures of crystalline Mg sulfates, but amorphous Mg sulfates may be present (Clark et al., 2022; Rampe et al., 2022). Future analysis of data from these traverse sections will address questions related to the environmental change that is hypothesized to be recorded in Mount Sharp as well as questions related to the pediment and activity in Gale crater that occurred after the deposition and erosion of Mount Sharp.

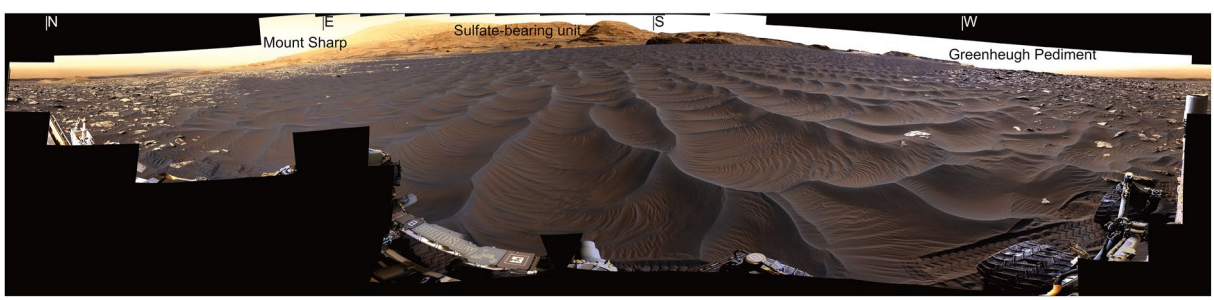

Figure 23. Mastcam 360° mosaic (2991MO15588, NASA/JPL-Caltech/MSSS) acquired on sol 2991 from the edge of the "Sands of Forvie" basaltic sand deposit. The center of the mosaic looks south from the rover position toward the sulfate-bearing unit. Rover wheels are approximately 40 cm wide and the distance across the sand to the south is about 235 m. See Figure 22 for orbital context.

Figure 24. Mastcam mosaic (3040ML15879, NASA/JPL-Caltech/MSSS) acquired on Sol 3040 looking west toward Mont Mercou, in the center of the image. The last drill sample (Nontron) of the Glen Torridon campaign was collected near the base of the exposed cliff face, which is approximately 6 m tall, before the rover ascended to the top of the escarpment to continue exploration of the transition to the sulfate-bearing unit.

5. Synthesis of Key Findings From Glen Torridon

5.1. The Sedimentary Facies Within Glen Torridon Record a General Transition From Predominately Lacustrine Mudstones to Interbedded Fluvial Sandstones

As described previously, the Glen Torridon region is defined by three stratigraphic members, including the Jura member of the Murray formation and the Knockfarril Hill and Glasgow members of the Carolyn Shoemaker formation (Fedo et al., 2022). At elevations below Glen Torridon, the Mount Sharp group generally consisted of laminated mudstones interpreted as lacustrine deposits, with only localized intervals of isolated sandstone beds indicating episodic occurrences of higher energy rivers within the overall quiet lacustrine setting (e.g., hyperpycnal flows, Stack et al., 2019). Starting in the Glen Torridon sedimentary succession, we observe more frequent occurrences of sand-rich deposits within the Jura member, progressively giving way to more frequent and widespread up-section cross-bedded sandstones of the Knockfarill Hill (Caravaca et al., 2022; Fedo et al., 2022), thus recording a transition to higher-energy fluvially influenced environments. This transition is marked by the interfingering between finer- and coarser-grained facies of the Jura and Knockfarril Hill members, respectively, but also the spatially "patchy" distribution of the sandstone-bearing outcrops, most notably within the Visionarium region (Figure 5) (Caravaca et al., 2022). This change in depositional setting is notable given that the Murray formation lacustrine deposits are more than 300 m thick, indicating prolonged lakebed deposition. The fluctuations in the crater's lake base level suggests a profound environmental shift in the history of Gale crater.

5.2. Glen Torridon Hosts the Highest Clay Mineral Abundances Observed Thus Far in Gale Crater, Though Measurements Remain in Family With the Rest of the Mount Sharp Group

Clay mineral abundances in typical Glen Torridon bedrock range between 34 wt % to 24 wt % at the Glen Etive and Glasgow drill holes, respectively (Thorpe et al., 2022). Lower clay mineral abundances were detected in the compositionally anomalous drill hole Hutton (~6 wt. %). Although Glen Etive is the most clay mineral-rich sample drilled thus far, in general the clay mineral abundances in Glen Torridon are in family with previous samples from the Mount Sharp group that were investigated before the clay mineral-poor Vera Rubin ridge (Achilles et al., 2020; Bristow et al., 2018; Rampe, Blake, et al., 2020; Rampe, Bristow, et al., 2020; Thorpe et al., 2022). They are also comparable to abundances detected in Bradbury Group rocks of the Yellowknife Bay region (Vaniman et al., 2014). Before Glen Torridon, the drill sample with the highest clay mineral abundance was Marimba, which had 28 wt. % phyllosilicates (Achilles et al., 2020; Bristow et al., 2018). The relative proportion of dioctahedral to trioctahedral smectites has been increasing as *Curiosity* has ascended Mount Sharp (Bristow et al., 2018), and Glen Torridon continues this trend with primarily dioctahedral smectites that indicate the smectites formed in an open geochemical system (Thorpe et al., 2022). H_2O released during SAM EGA also supports the presence of Fe-rich dioctahedral phyllosilicates in all Glen Torridon samples, corroborating CheMin detections (McAdam et al., 2022). While the reason for this relative enrichment in Fe^{3+} in Glen Torridon clays is still unclear, Bristow et al. (2021) hypothesize it could be related to a change in provenance of detrital materials.

Other rover observations provide additional support that clay minerals are present throughout Glen Torridon beyond the specific drill locations. Visible to near infrared (VNIR) spectra from Mastcam that are consistent with the presence of Fe^{3+}-bearing or Fe-/Mg-smectites occur in all stratigraphic members in Glen Torridon (Rudolph et al., 2022). The smectite signatures were strongest in the Jura and Knockfarril Hill members, slightly weaker in the Glasgow member, and disappeared in the Hutton interval (Rudolph et al., 2022). The DAN instrument was used to estimate the WEH, which uses the amount of hydrogen detected to estimate how much water could be present, along *Curiosity*'s traverse. The WEH is relatively low on Vera Rubin ridge, where the clay mineral abundances were low, and increased once the rover entered Glen Torridon, which supports the inference that clay minerals documented in drill samples are representative of bulk bedrock measured throughout Glen Torridon by DAN (Czarnecki et al., 2022). Additionally, the CIA and the abundance of Li obtained from the ChemCam instrument, which can be related to the amount of clay minerals, are elevated overall across Glen Torridon compared to the Vera Rubin ridge (Bristow et al., 2021; Dehouck et al., 2022). These elevated values are comparable to observations from other phyllosilicate bearing parts of Mount Sharp group (Mangold et al., 2019). All these observations are consistent with clay minerals making up a significant portion of the rocks in Glen Torridon, with the highest abundances in the Jura and Knockfarril Hill members.

5.3. Orbital Versus In-Situ Views: Orbital Observations of Glen Torridon Generally Reflect Secondary Processes and Surficial Expression, Rather Than Primary Processes

The Glen Torridon region was identified as a high priority field site in part because phyllosilicate minerals could be detected in the region by orbital spectroscopy, enabling predictions about the past aqueous environment. *Curiosity*'s science activities in Glen Torridon were designed to test hypotheses developed from orbital analyses of the geology and surface properties, as well as experience gained during the rover's preceding traverse. The complementary analyses of the regional patterns from orbit together with localized in-situ observations enabled greater contextualization of the smectite mineral detections in Glen Torridon, the linear ridge features, and the role of diagenesis and secondary processes.

In orbital data sets, Vera Rubin ridge and Glen Torridon are both mineralogically and morphologically distinct, yet *Curiosity* observations demonstrate the regions are stratigraphically equivalent and the distinct properties are interpreted as a result of different overprinting diagenetic histories (Fedo et al., 2020). In both of these regions, the mineralogy detected by CRISM is reflected in the assemblages detected by CheMin (Rampe, Bristow, et al., 2020), in that Vera Rubin ridge is generally depleted in phyllosilicates and lower Glen Torridon lacks significant iron oxides. Comparisons between spectra from CRISM and laboratory studies of desiccated smectites further confirm mineral detections and improve the ability to extrapolate beyond individual drill holes using orbital data sets (He et al., 2022). However, both hematite and phyllosilicates are common in in-situ sampling outside of regions where they are detected from orbit. VNIR reflectance spectroscopy only samples a few microns deep at the surface, so sand and dust cover strongly influence orbital VNIR mineral detections. Glen Torridon, particularly in the lower Jura strata, is the least dusty site visited by *Curiosity*, as determined by APXS elemental deconvolutions (i.e., VanBommel et al., 2016). The physical weathering of the surface is also inferred to enhance spectral retrievals; the strongest smectite signatures in CRISM data correspond to both the lack of dust (He et al., 2022) and also the "rubbly," highly eroded surfaces with locally derived regolith (Hughes, 2022). Similar associations between strong hematite signatures and fractured surfaces were observed at Vera Rubin ridge. Therefore, the fact that smectites can be detected in Glen Torridon by CRISM is likely to be a result of the surface being relatively dust- and sand-free (He et al., 2022).

5.4. The Most Clay Mineral-Rich Areas in Glen Torridon Experienced a Lower Degree of Diagenetic Modification Than the Surrounding Terrain

Diagenetic indicators (i.e., diagenetic features and chemical fractionation) are present across Glen Torridon, but they vary across the trough in ways that lead to constraints on the degree of post-depositional alteration that occurred. Diagenesis is the main contributor to the differences between the Jura member that outcrops on Vera Rubin ridge as compared to the Jura member that outcrops in Glen Torridon. Vera Rubin ridge records an extensive history of diagenesis: it is well-cemented (leading to very hard, ridge-forming rocks) and contains a variety

of diagenetic indicators ranging from veins and nodules to color variations that crosscut the stratigraphy (Bennett et al., 2021; Fraeman, Edgar, et al., 2020; Horgan et al., 2020; L'Haridon et al., 2020). The equivalent strata in the Jura that occurs in Glen Torridon, as well as strata within the Knockfarril Hill member, do not appear to have experienced the same diagenetic events; generally, these rocks do not contain many diagenetic features and they are softer and recessive compared to Vera Rubin ridge (Gasda et al., 2022; Rudolph et al., 2022).

Diagenesis can also explain the differences in mineralogy between Vera Rubin ridge and Glen Torridon. Glen Torridon samples have clay mineral contents of 24–34 wt. %, while Vera Rubin ridge samples only have clay minerals contents of 5–13 wt. % (Bristow et al., 2021; Rampe, Blake, et al., 2020; Rampe, Bristow, et al., 2020; Thorpe et al., 2022). The opposite trend is observed with iron oxides and oxyhydroxide abundances: Glen Torridon has <2 wt. % while Vera Rubin ridge has 9–16 wt. % (Bristow et al., 2021). These observations support the hypothesis that Vera Rubin ridge has a different diagenetic history than Glen Torridon, and the diagenetic fluids that increased the amount of iron oxides, cemented the ridge, and depleted the clay mineral abundances in Vera Rubin ridge did not affect the adjacent strata in Glen Torridon to the same extent. Additionally, Gasda et al. (2022) propose that because siderite is unstable and can be easily replaced by iron oxides, such as the ones on Vera Rubin ridge, the presence of siderite in Glen Torridon Jura and in Knockfarril Hill drill samples indicate that these strata experienced a different diagenetic history because it was not completely replaced.

Exceptions occur—along the base of Central butte in the Knockfarill Hill unit there are light-toned laminated sediments that are riddled with nodules (Bryk et al., 2020) and are crossed by numerous small veins (Gasda et al., 2022; Fedo et al., 2022; Rudolph et al., Rudolph et al., 2022). If this diagenetic modification added strength, it may have played some role in slowing the back wear of the erosional surface and the development of the butte. Facies within the Glasgow member also contain many morphologic, geochemical, and compositional diagenetic indicators. The low Zn concentrations measured by APXS associated with the upper Knockfarill Hill and Glasgow members relative to the rest of the Glen Torridon Mount Sharp group is also consistent with increased diagenesis within this region (O'Connell-Cooper et al., 2022). Within the Glasgow member, the anomalous Hutton interval bears evidence of a strong diagenetic overprint (Dehouck et al., 2022; O'Connell-Cooper et al., 2022; Thompson et al., 2022) and has a very low clay mineral abundance compared to the rest of Glen Torridon (6 wt. %; Thorpe et al., 2022), suggesting mineral recrystallization and post-depositional processes.

5.5. Habitability and Preservation of Organic Molecules: Glen Torridon Samples Have the Greatest Diversity and Abundance of Sulfur-Bearing Organics Thus Far Detected

SAM EGA and GCMS experiments conducted on Glen Torridon rocks yielded the greatest diversity and abundance of sulfur-bearing organics that *Curiosity* has detected thus far in the mission (Millan et al., 2022). The detection of new organic molecules extracted at high pyrolysis temperature (>600°C) and relatively high abundances of organics in Glen Torridon strata expanded the inventory of organic molecules identified in Gale crater sedimentary rocks but also supports the hypothesis that clay minerals on Mars played an important role in the preservation of ancient refractory organic matter. Finding evidence of ancient organic molecules indeed depends on the creation and concentration of those materials, but also the preservation. Diagenetic processes, particularly those involving oxidizing and acidic fluids, which are common throughout Martian history, are frequently destructive to biosignature preservation, even as they also provide elements of the necessary conditions for habitable environments. Fortunately, Glen Torridon proved to be an effective taphonomic window, having preserved abundant phyllosilicate minerals that are inferred to be relatively early alteration products and then remaining relatively unaffected by later processes.

SAM CO_2 and CO EGA data indicated the presence of oxidized organic compounds (e.g., oxalate salts) in addition to the reduced organic compounds in Glen Torridon samples, while the evolution of very little or no NO during EGA runs pointed to a lack or near lack of nitrate or nitrite salts in Glen Torridon samples. Sedimentary carbon, including organic molecules as detected by SAM, was present that could have supported a habitable environment, but a lack of significant indigenous N may have been a constraint on microbial activity (McAdam et al., 2022).

Further analysis of the SAM EGA results revealed that while the majority of Glen Torridon samples contained oxidized sulfur (largely as Fe sulfate), one Glen Torridon sample (Kilmarie) and one pediment sample (Edin-

burgh) showed evidence for minor amounts of reduced sulfur (Wong et al., 2022). The presence of both oxidized and reduced sulfur could indicate a complete sulfur redox cycle in Gale crater at this time. This could have supported the energetic needs of a hypothetical microbial ecosystem, increasing Glen Torridon's potential for ancient habitability (Wong et al., 2022).

5.6. The Anomalous Hutton Interval Likely Experienced Extensive Diagenesis

Within Glen Torridon, the Hutton interval in the Glasgow member stands out as an outcrop that has been diagenetically altered, likely more extensively than neighboring parts of the Glen Torridon region. The Hutton rocks display enrichments in several mobile elements, notably calcium, compared to the rest of Glen Torridon, resulting in lower CIA values (Dehouck et al., 2022). Such trends are inconsistent with the development of a weathering profile through percolation of dilute meteoric water, and instead point toward the circulation of concentrated diagenetic fluids (Dehouck et al., 2022).

The Hutton interval's location below the unconformable contact between the Mount Sharp group and the Siccar Point group suggests the diagenesis could be related to the unconformity. This hypothesis is supported by the observation that targets that are within 1–3 m of capping rocks at Western butte and in the Pahrump Hills and Hartmann's Valley members also show similar color, compositional and mineralogical trends (Thompson et al., 2022). The extensive diagenetic history at Vera Rubin ridge is also hypothesized to have been related to the once more extensive coverage of the Stimson formation, such that the capping rock may have provided pathways for fluid activity (Rampe, Bristow, et al., 2020; Thompson et al., 2020). The Hutton, Telegraph Peak, Buckskin, and Highfield Mount Sharp group drill samples all have clay mineral abundances less than 6 wt. %, and all have been interpreted to be located just below the contact with the Stimson formation. Additionally, Hutton, Telegraph Peak, and Buckskin are the only Mount Sharp drill samples where magnetite is the dominant Fe-oxide phase, suggesting diagenetic alteration occurred along the unconformity across the region.

If the diagenesis occurred in association with the unconformity, this alteration could have occurred either before or after the Stimson was deposited and lithified. The Stimson does not exhibit similar diagenetic features as the underlying Hutton interval, which could indicate that the fluids that altered the Hutton interval did not interact with the Stimson. Alternatively, the Hutton interval is depleted in sulfur, while targets in the Stimson closest to the unconformity are enriched in sulfur, and the Edinburgh drill sample is inferred to contain reduced sulfur (Wong et al., 2022). Sulfur could have been mobilized within the Hutton interval, and then precipitated in the Stimson sandstone that immediately overlies the contact (Thompson etal., 2022). This could suggest that the capping unit was present during this diagenetic event(s) and the unconformity may have acted as a conduit for the fluid (Bedford et al., 2022; Rudolph et al., 2022; Thompson et al., 2022). As a caveat, Gasda et al. (2022) notes that the diagenetic features (specifically the dark-toned veins and Mg-rich linear features) that occur within the Hutton interval are not observed elsewhere, which could suggest that a highly localized fluid event altered this area and that at least some diagenesis in the Hutton interval may be unrelated to the nearby unconformity. Multiple, complex fluid events are likely, and hypotheses regarding the Hutton interval can be further tested when *Curiosity*'s traverse revisits the Greenheugh pediment further upslope Mount Sharp.

5.7. The Greenheugh Pediment Is Capped by the Stimson Formation, Which Increases the Known Spatial Extent of This Sandstone Unit That Unconformably Overlies the Mount Sharp Group Rocks

Curiosity has now encountered the Siccar Point group multiple times along its traverse, indicating the past presence of an extensive aeolian sandstone deposit overlying the Mount Sharp group deposits. The multiple episodes of diagenesis required to cement these sandstones, as well as the indication of geochemical alteration along the contact with the underlying Mount Sharp group, demonstrate that subsurface liquid water was present in Gale crater after the deposition and erosion of Mount Sharp and the Stimson sandstones.

Stimson deposits at the Greenheugh pediment show similar aeolian driven cross bedding features that are broadly similar to previously encountered Stimson outcrops. Fluctuations in the sediment transport direction observed at Greenheugh pediment suggest wind regime variation at seasonal to millennial temporal scales (Banham et al., 2022). Contrasting sediment transport directions of the upper pediment sandstones versus the lower pediment and Emerson and Naukluft plateau Stimson deposits are consistent with their distinct compositions, as observed by APXS. Elevated K, Na, Mn, Fe, and Cr concentrations (relative to typical Stimson) are reflected in

the mineralogy of the pediment compared to previously drilled Stimson samples and are interpreted to reflect the incorporation of alkaline detritus. The alkaline material would have been sourced from a different area than the basaltic sand that comprises typical Stimson formation sandstone (Thompson et al., 2022). ChemCam data indicates that the pediment Stimson exhibits a distinct mafic signature that could suggest sediments were sourced from a local, olivine-rich source such as the mafic beds detected farther up the slopes of Mt Sharp (Bedford et al., 2022).

6. The Geologic History of Glen Torridon

The sedimentary rocks that now outcrop in Glen Torridon were originally deposited as part of the Mount Sharp group succession and consist of laminated mudstones deposited in lacustrine environments and local interbeds of fluvial deposits (Caravaca et al., 2022; Fedo et al., 2022). Further deposition of Mount Sharp strata occurred such that the Glen Torridon sediment was buried by an unknown (but possibly up to several kilometers thick) overburden (Lewis et al., 2019; Malin & Edgett, 2000). Lithification of the Glen Torridon strata occurred before the onset of the net erosion of the north face of Mount Sharp (Dehouck et al., 2022; Rudolph et al., 2022; Thorpe et al., 2022). Erosion of the lower Mount Sharp slopes generated the basal Siccar Point group unconformity, expressed as an erosional surface that was then preserved by deposition of an overlying aeolian sand dune deposit. The lithified sandstones, the Stimson formation, formed an erosion resistant cap on the basal Siccar Point group unconformity (Banham et al., 2022). Diagenetic events may have impacted the Mount Sharp group rocks that were closest to the basal Siccar Point group unconformity, such that the rocks at Vera Rubin ridge became better-cemented than the surrounding areas and the Hutton interval was diagenetically altered and perhaps "recharged" in mobile elements (Bedford et al., 2022; Thompson et al., 2022). Subsequent wind erosion caused escarpment retreat of the pediment-capping unit and vertical incision in the less resistant underlying rocks, leading to the isolated plateaus and buttes near the base of Mt Sharp, the emergence of Vera Rubin ridge, and the 10 m high modern escarpment edge which defined the northern boundary of the Greenheugh pediment. A long term, steady wind regime sculpted the softer Mount Sharp group rocks within Glen Torridon into the highly eroded, ridged surface expression that is observed today (Hughes, 2022; Stack et al., 2022, Sullivan et al., 2022; Weitz et al., 2022).

Overall, throughout their history, strata within Glen Torridon experienced alteration from groundwater fluids of variable redox potential, chemistry, pH, and water-to-rock ratios (McAdam et al., 2022). This is evidence for a dynamic subsurface environment within Gale crater, but also makes it challenging to determine a unique series of diagenetic events or processes. However, several constraints can be placed on the timing of events in Glen Torridon. First, the formation of phyllosilicates in Glen Torridon likely occurred early, either as detrital inputs or as syn-depositional alteration products (Dehouck et al., 2022; Thorpe et al., 2022). The Fe-carbonates also likely precipitated relatively early during diagenesis, possibly via groundwater mixing that may have included brines (Bristow et al., 2021; Thorpe et al., 2022). The SAM instrument may have detected trace amounts of Fe-carbonate in Vera Rubin ridge samples (CheMin did not detect any), which suggests that this fluid may have also permeated Vera Rubin ridge strata (McAdam et al., 2020). Sometime after this, a diagenetic event that impacted Vera Rubin ridge led to the reduction of clays and Fe-carbonates (if the latter was present), an increase in crystalline hematite, and the recrystallization and enhanced cementation of the ridge (Bristow et al., 2021; Rampe, Blake, et al., 2020; Rampe, Bristow, et al., 2020). This event was likely relatively late in Mount Sharp's history (possibly associated with the formation of the basal Siccar Point unconformity) and did not significantly impact Glen Torridon strata. The diagenetic event that affected the Hutton interval was also late (and possibly was related to the event that affected Vera Rubin ridge), and likely associated with the basal Siccar Point unconformity.

7. Summary and Major Conclusions From the Glen Torridon Campaign

Curiosity's successful campaign in Glen Torridon addressed several overarching science questions about the region. The science questions and answers to those questions are summarized here:

Campaign question 1: *What is the stratigraphic context of rocks exposed in Glen Torridon, and what was the primary depositional process(es)?* Strata in Glen Torridon form part of the Mount Sharp group. The base of the sedimentary succession in Glen Torridon is stratigraphically equivalent to the Jura member within Vera Rubin ridge, despite mineralogical differences due to post-depositional diagenesis. These sedimentary rocks represent a

continuation of the lacustrine environments of the Murray formation. The widespread presence of cross-bedded sandstones in strata overlying the Jura member and a distinct transition from laminated mudstones led to the designation of the Knockfarril Hill member in a new formation, the Carolyn Shoemaker formation. The Knockfarril Hill member may record lake margin fluvial deposits. The Glasgow member, which overlies the Knockfarril Hill member, records a return to lacustrine sedimentation but is marked by strong diagenetic overprinting. The pediment capping unit unconformably overlies Carolyn Shoemaker formation deposits in Glen Torridon and is interpreted to be part of the Stimson formation (Siccar Point group), an aeolian cross-stratified sandstone unit that was deposited later in Gale crater's history.

Campaign question 2: *How did post-depositional processes contribute to the geologic history of the region?* Diagenesis was heterogenous across Glen Torridon, with zones of enhanced diagenesis (i.e., the Hutton interval) and areas where diagenesis is relatively minor. The most clay-rich areas in Glen Torridon likely experienced less diagenesis than the surrounding terrain, such that the phyllosilicates and organic molecules are relatively better preserved. Glen Torridon hosts the highest clay mineral abundances observed thus far in Gale crater, but it remains in family with the rest of the Mount Sharp group with clay mineral abundances that are only ∼6 wt. % higher than some previous samples. The CRISM reflectance spectral signatures in the Glen Torridon area are consistent with the clay minerals measured in-situ, and the spatial distribution of orbital measurements likely reflect a combination of the prevalence of clay minerals and the erosional environment in the trough that keeps surfaces relatively dust free. Post-depositional differential strengthening of rocks in the area surrounding Glen Torridon as a result of diagenesis led wind erosion to etch out the Glen Torridon trough, creating Vera Rubin ridge, isolated mesas, and the sharp pediment escarpment. In general, orbital observations of Glen Torridon tend to reflect the style of surficial expression and exposure of rocks, rather than primary processes. Particularly, the NE/SW trending ridges identified from orbit are interpreted to be erosional features rather than primary depositional features.

Campaign question 3: *What are the implications for habitability of Glen Torridon strata, particularly for the preservation of organic molecules?* Glen Torridon samples show the greatest diversity and abundance of sulfur-bearing organics thus far detected in Gale crater. Given that Glen Torridon strata contain abundant clay minerals, this supports the hypothesis that clay minerals have a high preservation potential for organic molecules. Sedimentary carbon present in the deposits could have supported habitable environments. Additionally, the presence of both oxidized and reduced sulfur could indicate a complete sulfur redox cycle that could have supported the energetic needs of a hypothetical microbial ecosystem. Although the lack of N may have provided a constraint, the combination of evidence for water, organic C, and redox sensitive elements indicates that the sedimentary environment represented by Glen Torridon strata was a potentially habitable environment.

Broader applications to Mars: In addition to answering specific campaign questions, the results from Glen Torridon have broader applications to Mars. The body of work summarized here characterizes the clay-bearing strata within Mount Sharp that outcrops just below sulfate-bearing strata. These results characterizing the depositional environments, aqueous history, and habitability of the Glen Torridon area will enable future studies that focus on the transition between the clay- and sulfate-bearing strata to test the hypothesis that this represents a global climatic shift on Mars. Glen Torridon records the transition from Mount Sharp strata that was deposited in a lacustrine environment to strata that was deposited in a more energetic fluvial environment, and future analyses can investigate whether this marks the start of a shift to different depositional environments.

These findings contribute to our ability to interpret features identified from orbital data sets. Glen Torridon showed that features observable from orbit (geomorphology, mineralogy) can be a result of secondary processes related to diagenesis and erosion, suggesting that caution must be exercised when attempting to constrain primary depositional processes.

The aqueous environments identified in Glen Torridon strata provide further evidence of ancient habitable environments and water on the surface of Mars. Results from Glen Torridon offer evidence that clay minerals can have a high organic preservation potential on Mars, so clay mineral-rich aqueous deposits (here observed as both lacustrine and fluvial deposits) could be good future targets for searching for ancient habitable environments on Mars and organics. Finally, identifying ancient organic molecules and aqueous environments reinforces our understanding that Mars has hosted many habitable environments in the past.

Data Availability Statement

All Mars Science Laboratory data described in this manuscript are available at the Planetary Data System Geosciences Node (https://pds-geosciences.wustl.edu/missions/msl/index.htm). This includes data sets from APXS (Gellert, 2012), MAHLI (Edgett, 2013a, 2013b), Mastcam (Malin, 2013), ChemCam (Wiens, 2013a, 2013b), CheMin (Vaniman, 2013), SAM (Mahaffy, 2013), and DAN (Mitrofanov, 2012). Derived data products that were mentioned in the manuscript are available via the cited manuscripts (i.e., the other manuscripts submitted to this special issue). HiRISE (McEwen, 2005) and CTX (Malin, 2007) data used for figure backgrounds are also available at the Planetary Data System Geosciences Node (https://pds-geosciences.wustl.edu/missions/mro/default.htm).

Acknowledgments
The authors would like to thank the entire Mars Science Laboratory (MSL) team for their hard work on this campaign, including transitioning to fully remote operations for the first time in the middle of the campaign to respond to the global pandemic in 2020. Funding from the MSL was used to conduct this work. The Mastcam mosaics included in figures were produced by the Mastcam science and operations team at Malin Space Science Systems. The authors would like to thank Sanjeev Gupta and an anonymous reviewer for their helpful comments that improved the manuscript. A portion of this research was carried out at the Jet Propulsion Laboratory, California Institute of Technology, under a contract with the National Aeronautics and Space Administration (80NM0018D0004).

References

Achilles, C. N., Rampe, E. B., Downs, R. T., Bristow, T. F., Ming, D. W., Morris, R. V., et al. (2020). Evidence for multiple diagenetic episodes in ancient fluvial-lacustrine sedimentary rocks in Gale Crater, Mars. *Journal of Geophysical Research: Planets*, *125*(8), e2019JE006295. https://doi.org/10.1029/2019JE006295

Anderson, R., & Bell, J. F. (2010). Geologic mapping and characterization of Gale Crater and implications for its potential as a Mars Science Laboratory landing site. *The Mars Journal*, *5*, 76–128. https://doi.org/10.1555/mars.2010.0004

Banham, S. G., Gupta, S., Rubin, D. M., Edgett, K. S., Barnes, R., Van Beek, J., et al. (2021). A rock record of complex aeolian bedforms in a Hesperian Desert landscape: The Stimson formation as exposed in the Murray buttes, Gale Crater, Mars. *Journal of Geophysical Research: Planets*, *126*(4), e2020JE006554. https://doi.org/10.1029/2020JE006554

Banham, S. G., Gupta, S., Rubin, D. M., Bedford, C. C., Edgar, L., Bryk, A. B., et al. (2022). Evidence for seasonal- to millennial-scale wind fluctuations in an ancient aeolian dune field: Reconstruction of the Hesperian Stimson formation at Glen Torridon, Gale crater, Mars. *Journal of Geophysical Research: Planets*, *127*, e2021JE007023. https://doi.org/10.1029/2021JE007023

Banham, S. G., Gupta, S., Rubin, D. M., Watkins, J. A., Sumner, D. Y., Edgett, K. S., et al. (2018). Ancient Martian aeolian processes and palaeomorphology reconstructed from the Stimson formation on the lower slope of Aeolis Mons, Gale crater, Mars. *Sedimentology*, *65*(4), 993–1042. https://doi.org/10.1111/sed.12469

Bedford, C. C., Banham, S. G., Bridges, J. C., Forni, O., Cousin, A., Bowden, D., et al. (2022). An insight into ancient aeolian processes and post-Noachian aqueous alteration in Gale crater, Mars, using ChemCam geochemical data from the Greenheugh capping unit. *Journal of Geophysical Research: Planets*, *127*, e2021JE007100. https://doi.org/10.1029/2021JE007100

Bedford, C. C., Schwenzer, S. P., Bridges, J. C., Banham, S., Wiens, R. C., Gasnault, O., et al. (2020). Geochemical variation in the Stimson formation of Gale crater: Provenance, mineral sorting, and a comparison with modern Martian dunes. *Icarus*, *341*, 113622. https://doi.org/10.1016/j.icarus.2020.113622

Bell, J. F., III, Godber, A., McNair, S., Caplinger, M. A., Maki, J. N., Lemmon, M. T., et al. (2017). The Mars Science Laboratory Curiosity rover Mastcam instruments: Preflight and in-flight calibration, validation, and data archiving. *Earth and Space Science*, *4*(7), 396–452. https://doi.org/10.1002/2016EA000219

Bennett, K. A., Fox, V. K., Vasavada, A. R., Grotzinger, J., Edwards, C. S., & Science Team, M. S. L. (2018). The clay-bearing unit in Gale Crater II: Plans for the investigation of the clay-bearing unit by the Curiosity rover. *Presented at the 49th Lunar and Planetary Science Conference* (Vol. #1277). Retrieved from https://www.hou.usra.edu/meetings/lpsc2018/pdf/1277.pdf

Bennett, K. A., Hill, J. R., Murray, K. C., Edwards, C. S., Bell, J. F., III, & Christensen, P. R. (2018). THEMIS-VIS investigations of sand at Gale Crater. *Earth and Space Science*, *5*(8), 352–363. https://doi.org/10.1029/2018EA000380

Bennett, K. A., Rivera-Hernández, F., Tinker, C., Horgan, B., Fey, D. M., Edwards, C., et al. (2021). Diagenesis revealed by fine-scale features at Vera Rubin ridge, Gale Crater, Mars. *Journal of Geophysical Research: Planets*, *126*(5), e2019JE006311. https://doi.org/10.1029/2019JE006311

Bibring, J.-P., Langevin, Y., Gendrin, A., Gondet, B., Poulet, F., Berthé, M., et al. (2005). Mars surface diversity as revealed by the OMEGA/Mars express observations. *Science*, *307*(5715), 1576–1581. https://doi.org/10.1126/science.1108806

Bibring, J.-P., Langevin, Y., Mustard, J. F., Poulet, F., Arvidson, R., Gendrin, A., et al. (2006). Global mineralogical and aqueous Mars history derived from OMEGA/Mars express data. *Science*, *312*(5772), 400–404. https://doi.org/10.1126/science.1122659

Bishop, J. L., Dobrea, E. Z. N., McKeown, N. K., Parente, M., Ehlmann, B. L., Michalski, J. R., et al. (2008). Phyllosilicate diversity and past aqueous activity revealed at Mawrth Vallis, Mars. *Science*, *321*(5890), 830–833. https://doi.org/10.1126/science.1159699

Blake, D., Vaniman, D., Achilles, C., Anderson, R., Bish, D., Bristow, T., et al. (2012). Characterization and calibration of the CheMin mineralogical instrument on Mars Science Laboratory. *Space Science Reviews*, *170*(1), 341–399. https://doi.org/10.1007/s11214-012-9905-1

Bristow, T. F., Bish, D. L., Vaniman, D. T., Morris, R. V., Blake, D. F., Grotzinger, J. P., et al. (2015). The origin and implications of clay minerals from Yellowknife Bay, Gale crater, Mars. *American Mineralogist*, *100*(4), 824–836. https://doi.org/10.2138/am-2015-5077CCBYNCND

Bristow, T. F., Grotzinger, J. P., Rampe, E. B., Cuadros, J., Chipera, S. J., Downs, G. W., et al. (2021). Brine-driven destruction of clay minerals in Gale crater, Mars. *Science*, *373*(6551), 198–204. https://doi.org/10.1126/science.abg5449

Bristow, T. F., Rampe, E. B., Achilles, C. N., Blake, D. F., Chipera, S. J., Craig, P., et al. (2018). Clay mineral diversity and abundance in sedimentary rocks of Gale crater, Mars. *Science Advances*, *4*(6), eaar3330. https://doi.org/10.1126/sciadv.aar3330

Bryk, A. B., Dietrich, W. E., Fox, V. K., Bennett, K. A., Banham, S. G., Lamb, M. P., et al. (2020). The stratigraphy of Central and Western Butte and the Greenheugh Pediment Contact (p. Abstract #2612). In *51st Lunar and Planetary Science Conference*. Lunar and Planetary Institute. Retrieved from https://www.hou.usra.edu/meetings/lpsc2020/pdf/2612.pdf

Calef, F. J., III, & Parker, T. (2016). *MSL Gale merged orthophoto mosaic*. PDS Annex. U.S. Geological Survey. Retrieved from http://bit.ly/MSL_Basemap

Caravaca, G., Mangold, N., Dehouck, E., Schieber, J., Zaugg, L., Bryk, A. B., et al. (2022). From lake to river: Documenting an environmental transition across the Jura/Knockfarril Hill members boundary in the Glen Torridon region of Gale crater (Mars). *Journal of Geophysical Research: Planets*, *127*, e2021JE007023. https://doi.org/10.1029/2021JE007093

Christian, J. R., Arvidson, R. E., O'Sullivan, J. A., Vasavada, A. R., & Weitz, C. M. (2022). CRISM-Based high spatial resolution thermal inertia mapping along Curiosity's traverses in Gale Crater. *Journal of Geophysical Research: Planets*, *127*, e2021JE007076. https://doi.org/10.1029/2021JE007076

Clark, J. V., Sutter, B., Wong, G., Lewis, J., McAdam, A., Archer, P. D., et al. (2022). Sample analysis at Mars-Evolved Gas analysis (SAM-EGA) results from the clay-sulfate transition region in Gale Crater, Mars. *53rd LPSC*.

Czarnecki, S., Hardgrove, C., Arvidson, R. E., Hughes, M. N., Schmidt, M. E., Henley, T., et al. (2022). Hydration of a clay-rich unit on Mars, comparison of orbital data to rover data. *Journal of Geophysical Research: Planets*, *127*, e2021JE007104. https://doi.org/10.1029/2021JE007104

Dehouck, E., Cousin, A., Mangold, N., Frydenvang, J., Gasnault, O., Forni, O., et al. (2022). Bedrock geochemistry and alteration history of the clay-bearing Glen Torridon region of Gale crater, Mars. *Journal of Geophysical Research: Planets*, *127*, e2021JE007103. https://doi.org/10.1029/2021JE007103

Edgar, L. A., Fedo, C. M., Gupta, S., Banham, S. G., Fraeman, A. A., Grotzinger, J. P., et al. (2020). A lacustrine paleoenvironment recorded at Vera Rubin ridge, Gale Crater: Overview of the sedimentology and stratigraphy observed by the Mars Science Laboratory Curiosity rover. *Journal of Geophysical Research: Planets*, *125*(3), e2019JE006307. https://doi.org/10.1029/2019JE006307

Edgett, K. S. (2013a). MSL Mars Hand Lens Imager 2 EDR image V1.0 [Dataset]. NASA Planetary Data System. https://doi.org/10.17189/1520187

Edgett, K. S. (2013b). MSL Mars Hand Lens Imager 2 EDR zstack V1.0 [Dataset]. NASA Planetary Data System. https://doi.org/10.17189/1520396

Edgett, K. S., Yingst, R. A., Ravine, M. A., Caplinger, M. A., Maki, J. N., Ghaemi, F. T., et al. (2012). Curiosity's Mars Hand Lens Imager (MAHLI) investigation. *Space Science Reviews*, *170*(1–4), 259–317. https://doi.org/10.1007/s11214-012-9910-4

Ehlmann, B. L., & Buz, J. (2015). Mineralogy and fluvial history of the watersheds of Gale, Knobel, and sharp craters: A regional context for the Mars Science Laboratory Curiosity's exploration. *Geophysical Research Letters*, *42*(2), 264–273. https://doi.org/10.1002/2014GL062553

Ehlmann, B. L., Mustard, J. F., Murchie, S. L., Bibring, J.-P., Meunier, A., Fraeman, A. A., & Langevin, Y. (2011). Subsurface water and clay mineral formation during the early history of Mars. *Nature*, *479*(7371), 53–60. https://doi.org/10.1038/nature10582

Eigenbrode, J. L., Summons, R. E., Steele, A., Freissinet, C., Millan, M., Navarro-González, R., et al. (2018). Organic matter preserved in 3-billion-year-old mudstones at Gale crater, Mars. *Science*, *363*(6393), 1096–1101. https://doi.org/10.1126/science.aas9185

Fedo, C. M., Bryk, A. B., Edgar, L. A., Bennett, K. A., Fox, V. K., Dietrich, W. E., et al. (2022). Stratigraphic-based bedrock geologic map of the Murray and Carolyn Shoemaker formations along the traverse of the *Curiosity* rover. *Journal of Geophysical Research: Planets*, *127*, e2022JE007408. https://doi.org/10.1029/2022JE007408

Fedo, C. M., Grotzinger, J. P., Bryk, A., Bennett, K., Fox, V., Stein, N., et al. (2020). Ground-based stratigraphic correlation of the Jura and Knockfarril Hill members of the Murray formation, Gale crater: Bridging the Vera Rubin ridge – Glen Torridon divide. In *51st Lunar and Planetary Science Conference* (p. 2345). Lunar & Planetary Institute. Retrieved from https://hal.archives-ouvertes.fr/hal-02526528

Fedo, C. M., Grotzinger, J. P., Gupta, S., Fraeman, A., Edgar, L., Edgett, K., et al. (2018). Sedimentology and stratigraphy of the Murray formation, Gale Crater, Mars, 2078. *Presented at the 49th Annual Lunar and Planetary Science Conference*.

Fox, V. K., Bennett, K. A., Vasavada, A. R., Stack, K. M., & Ehlmann, B. L. (2018). The clay-bearing unit of Mount sharp, Gale Crater, I: Orbital perspective and initial results (p. Abstract #1728). *Presented at the 49th Lunar and Planetary Science Conference*, Lunar and Planetary Institute. Retrieved from https://www.hou.usra.edu/meetings/lpsc2018/pdf/1728.pdf

Fox, V. K., Kupper, R. J., Ehlmann, B. L., Catalano, J. G., Razzell-Hollis, J., Abbey, W. J., et al. (2021). Synthesis and characterization of Fe(III)-Fe(II)-Mg-Al smectite solid solutions and implications for planetary science. *American Mineralogist*, *106*(6), 964–982. https://doi.org/10.2138/am-2020-7419CCBYNCND

Fraeman, A. A., Edgar, L. A., Rampe, E. B., Thompson, L. M., Frydenvang, J., Fedo, C. M., et al. (2020). Evidence for a diagenetic origin of Vera Rubin ridge, Gale Crater, Mars: Summary and synthesis of Curiosity's exploration Campaign. *Journal of Geophysical Research: Planets*, *125*(12), e2020JE006527. https://doi.org/10.1029/2020JE006527

Fraeman, A. A., Ehlmann, B. L., Arvidson, R. E., Edwards, C. S., Grotzinger, J. P., Milliken, R. E., et al. (2016). The stratigraphy and evolution of lower Mount Sharp from spectral, morphological, and thermophysical orbital data sets: Stratigraphy and evolution of Mount Sharp. *Journal of Geophysical Research: Planets*, *121*(9), 1713–1736. https://doi.org/10.1002/2016JE005095

Fraeman, A. A., Johnson, J. R., Arvidson, R. E., Rice, M. S., Wellington, D. F., Morris, R. V., et al. (2020). Synergistic ground and orbital observations of iron oxides on Mt. Sharp and Vera Rubin ridge. *Journal of Geophysical Research: Planets*, *125*(9), e2019JE006294. https://doi.org/10.1029/2019JE006294

Gasda, P. J., Comellas, J., Essunfeld, A., Das, D., Bryk, A. B., Dehouck, E., et al. (2022). Overview of the morphology and chemistry of diagenetic features in the clay-rich Glen Torridon unit of Gale Crater, Mars. *Journal of Geophysical Research: Planets*, *127*, e2021JE007097. https://doi.org/10.1029/2021JE007097

Gellert, R. (2012). MSL Mars alpha particle X-ray spectrometer 2 EDR V1.0 [Dataset]. NASA Planetary Data System. https://doi.org/10.17189/1519534

Gellert, R., & Clark, B. C., III, & MSL and MER Science Teams. (2015). In situ compositional measurements of rocks and soils with the alpha particle X-ray spectrometer on NASA's Mars rovers. *Elements*, *11*(1), 39–44. https://doi.org/10.2113/gselements.11.1.39

Goetz, W., Dehouck, E., Gasda, P. J., Johnson, J. R., Meslin, P.-Y, Lanza, N. L., et al. (2022). Detection of copper by the ChemCam instrument along *Curiosity*'s traverse in Gale crater, Mars: Elevated abundances in Glen Torridon. *Journal of Geophysical Research: Planets*, *128*, https://doi.org/10.1029/2021JE007101

Grotzinger, J. P., Crisp, J., Vasavada, A. R., Anderson, R. C., Baker, C. J., Barry, R., et al. (2012). Mars Science Laboratory mission and science investigation. *Space Science Reviews*, *170*(1–4), 5–56. https://doi.org/10.1007/s11214-012-9892-2

Grotzinger, J. P., Gupta, S., Malin, M. C., Rubin, D. M., Schieber, J., Siebach, K., et al. (2015). Deposition, exhumation, and paleoclimate of an ancient lake deposit, Gale crater, Mars. *Science*, *350*(6257), aac7575. https://doi.org/10.1126/science.aac7575

Grotzinger, J. P., & Milliken, R. E. (2012). The sedimentary rock record on Mars: Distribution, origins, and global stratigraphy. *Sedimentary Geology of Mars*, *102*, 1–48. https://doi.org/10.2110/pec.12.102.0001

Grotzinger, J. P., Sumner, D. Y., Kah, L. C., Stack, K., Gupta, S., Edgar, L., et al. (2014). A habitable fluvio-lacustrine environment at Yellowknife Bay, Gale Crater, Mars. *Science*, *343*(6169), 1242777. https://doi.org/10.1126/science.1242777

Gwizd, S. J., Fedo, C., Grotzinger, J., Edgett, K. S., Rivera-Hernández, F., Gupta, S., et al. (2020). Transition from a lacustrine margin to a lacustrine basin in Gale Crater, Mars: The Hartmann's Valley and Karasburg members of the Murray formation, 2719. *Presented at the 51st Annual Lunar and Planetary Science Conference*.

Hallet, B., Sletten, R. S., Malin, M., Mangold, N., Sullivan, R. J., Fairén, A. G., et al. (2022). Active ground patterns near Mars' equator in the Glen Torridon region of Gale Crater. *Journal of Geophysical Research: Planets*. https://doi.org/10.1029/2021je007126

He, L., Arvidson, R. E., O'Sullivan, J. A., Morris, R. V., Condus, T., Hughes, M. N., & Powell, K. E. (2022). Surface kinetic temperatures and nontronite single scattering albedo spectra from Mars reconnaissance orbiter CRISM hyperspectral imaging data over Glen Torridon, Gale Crater, Mars. *Journal of Geophysical Research: Planets*, *127*, e2021JE007092. https://doi.org/10.1029/2021JE007092

Horgan, B. H. N., Johnson, J. R., Fraeman, A. A., Rice, M. S., Seeger, C., Bell, J. F., III, et al. (2020). Diagenesis of Vera Rubin ridge, Gale Crater, Mars, from Mastcam multispectral images. *Journal of Geophysical Research: Planets*, *125*(11), e2019JE006322. https://doi.org/10.1029/2019JE006322

Hughes, M. (2022). Geomorphic map of Glen Torridon in Gale crater, Mars. *Digital Research Materials (Data & Supplemental files)*, *95*. Retrieved from https://openscholarship.wustl.edu/data/95

Hurowitz, J. A., Grotzinger, J. P., Fischer, W. W., McLennan, S. M., Milliken, R. E., Stein, N., et al. (2017). Redox stratification of an ancient lake in Gale crater, Mars. *Science*, *356*(6341), eaah6849. https://doi.org/10.1126/science.aah6849

Johnson, J. R., Bell, J. F., Bender, S., Blaney, D., Cloutis, E., Ehlmann, B., et al. (2016). Constraints on iron sulfate and iron oxide mineralogy from ChemCam visible/near-infrared reflectance spectroscopy of Mt. Sharp basal units, Gale Crater, Mars. *American Mineralogist*, *101*(7), 1501–1514. https://doi.org/10.2138/am-2016-5553

Johnson, S. S., Millan, M., Graham, H., Benison, K. C., Williams, A. J., McAdam, A., et al. (2020). Lipid biomarkers in ephemeral acid salt lake mudflat/sandflat sediments: Implications for Mars. *Astrobiology*, *20*(2), 167–178. https://doi.org/10.1089/ast.2017.1812

Khan, S., Stack, K., Aileen Yingst, R., & Bergmann, K. (2022). Characterization of clasts in the Glen Torridon region of Gale crater observed by the Mars Science Laboratory *Curiosity* Rover. *Journal of Geophysical Research: Planets*, *127*, e2021JE007095. https://doi.org/10.1029/2021JE007095

Lanza, N. L., Fischer, W. W., Wiens, R. C., Grotzinger, J., Ollila, A. M., Cousin, A., et al. (2014). High manganese concentrations in rocks at Gale crater, Mars. *Geophysical Research Letters*, *41*(16), 5755–5763. https://doi.org/10.1002/2014GL060329

Le Deit, L., Hauber, E., Fueten, F., Pondrelli, M., Rossi, A. P., & Jaumann, R. (2013). Sequence of infilling events in Gale Crater, Mars: Results from morphology, stratigraphy, and mineralogy: Sedimentary infilling in Gale crater. *Journal of Geophysical Research: Planets*, *118*(12), 2439–2473. https://doi.org/10.1002/2012JE004322

Lewis, K. W., Peters, S., Gonter, K., Morrison, S., Schmerr, N., Vasavada, A. R., & Gabriel, T. (2019). A surface gravity traverse on Mars indicates low bedrock density at Gale crater. *Science*, *363*(6426), 535–537. https://doi.org/10.1126/science.aat0738

L'Haridon, J., Mangold, N., Fraeman, A. A., Johnson, J. R., Cousin, A., Rapin, W., et al. (2020). Iron mobility during diagenesis at Vera Rubin ridge, Gale Crater, Mars. *Journal of Geophysical Research: Planets*, *125*(11), e2019JE006299. https://doi.org/10.1029/2019JE006299

Mahaffy, P. (2013). MSL Mars sample analysis at Mars 2 RDR level 0 V1.0 [Dataset]. NASA Planetary Data System. https://doi.org/10.17189/1519555

Mahaffy, P. R., Webster, C. R., Cabane, M., Conrad, P. G., Coll, P., Atreya, S. K., et al. (2012). The sample analysis at Mars investigation and instrument suite. *Space Science Reviews*, *170*(1), 401–478. https://doi.org/10.1007/s11214-012-9879-z

Malin, M. C. (2007). MRO context camera experiment data record level 0 V1.0 [Dataset]. NASA Planetary Data System. https://doi.org/10.17189/1520266

Malin, M. C. (2013). MSL Mars Mast Camera 2 EDR image V1.0 [Dataset]. NASA Planetary Data System. https://doi.org/10.17189/1520190

Malin, M. C., & Edgett, K. S. (2000). Sedimentary rocks of early Mars. *Science*, *290*(5498), 1927–1937. https://doi.org/10.1126/science.290.5498.1927

Malin, M. C., Ravine, M. A., Caplinger, M. A., Tony Ghaemi, F., Schaffner, J. A., Maki, J. N., et al. (2017). The Mars Science Laboratory (MSL) mast cameras and descent imager: Investigation and instrument descriptions. *Earth and Space Science*, *4*(8), 506–539. https://doi.org/10.1002/2016EA000252

Mangold, N., Dehouck, E., Fedo, C., Forni, O., Achilles, C., Bristow, T., et al. (2019). Chemical alteration of fine-grained sedimentary rocks at Gale crater. *Icarus*, *321*, 619–631. https://doi.org/10.1016/j.icarus.2018.11.004

Maurice, S., Wiens, R. C., Saccoccio, M., Barraclough, B., Gasnault, O., Forni, O., et al. (2012). The ChemCam instrument suite on the Mars Science Laboratory (MSL) rover: Science objectives and mast unit description. *Space Science Reviews*, *170*(1), 95–166. https://doi.org/10.1007/s11214-012-9912-2

McAdam, A. C., Sutter, B., Archer, P. D., Franz, H. B., Wong, G. M., Lewis, J. M. T., et al. (2020). Constraints on the mineralogy and geochemistry of Vera Rubin ridge, Gale Crater, Mars, from Mars Science Laboratory sample analysis at Mars Evolved Gas analyses. *Journal of Geophysical Research: Planets*, *125*(11), e2019JE006309. https://doi.org/10.1029/2019JE006309

McAdam, A. C., Sutter, B., Archer, P. D., Franz, H. B., Wong, G. M., Lewis, J. M. T., et al. (2022). Evolved gas analyses of sedimentary rocks from the Glen Torridon clay-bearing unit, Gale crater, Mars: Results from the Mars Science Laboratory Sample Analysis at Mars instrument suite. *Journal of Geophysical Research: Planets*, *127*, e2022JE007179. https://doi.org/10.1029/2022JE007179

McEwen, A. (2005). MRO Mars high resolution image science experiment EDR V1.0 [Dataset]. NASA Planetary Data System. https://doi.org/10.17189/1520179

McEwen, A. S., Eliason, E. M., Bergstrom, J. W., Bridges, N. T., Hansen, C. J., Delamere, W. A., et al. (2007). Mars reconnaissance orbiter's high resolution imaging science experiment (HiRISE). *Journal of Geophysical Research*, *112*(E5), E05S02. https://doi.org/10.1029/2005JE002605

McKay, C. P. (1996). Elemental composition, solubility, and optical properties of Titan's organic haze. *Planetary and Space Science*, *44*(8), 741–747. https://doi.org/10.1016/0032-0633(96)00009-8

Millan, M., Teinturier, S., Malespin, C. A., Bonnet, J. Y., Buch, A., Dworkin, J. P., et al. (2021). Organic molecules revealed in Mars's Bagnold Dunes by Curiosity's derivatization experiment. *Nature Astronomy*, 1–12. https://doi.org/10.1038/s41550-021-01507-9

Millan, M., Williams, A. J., Buch, A., Bai, A., Freissinet, C., Szopa, C., et al. (2018). Preservation of organic molecules in Mars-analog samples using pyrolysis and derivatization GCMS experiments from the SAM instrument. *49th LPSC Lunar and Planetary Science Conference 2018*. Retrieved from https://hal.archives-ouvertes.fr/hal-01815511

Millan, M., Williams, A. J., McAdam, A., Eigenbrode, J. L., Steele, A., Freissinet, C., et al. (2022). Characterization of organic molecules in the Glen Torridon region of Gale Crater, Mars, by the SAM instrument suite on board the *Curiosity* rover. *Journal of Geophysical Research: Planets*, *127*, e2021JE007107. https://doi.org/10.1029/2021JE007107

Milliken, R. E., Ewing, R. C., Fischer, W. W., & Hurowitz, J. (2014). Wind-blown sandstones cemented by sulfate and clay minerals in Gale Crater, Mars. *Geophysical Research Letters*, *41*(4), 1149–1154. https://doi.org/10.1002/2013GL059097

Milliken, R. E., Grotzinger, J. P., & Thomson, B. J. (2010). Paleoclimate of Mars as captured by the stratigraphic record in Gale Crater. *Geophysical Research Letters*, *37*(4), L04201. https://doi.org/10.1029/2009GL041870

Mitrofanov, I. (2012). MSL Mars dynamic albedo of neutrons 2 EDR V1.0 [Dataset]. NASA Planetary Data System. https://doi.org/10.17189/1519455

Mitrofanov, I. G., Litvak, M. L., Varenikov, A. B., Barmakov, Y. N., Behar, A., Bobrovnitsky, Y. I., et al. (2012). Dynamic Albedo of Neutrons (DAN) experiment onboard NASA's Mars Science Laboratory. *Space Science Reviews*, *170*(1), 559–582. https://doi.org/10.1007/s11214-012-9924-y

Mojarro, A., Williams, A. J., Millan, M., Eigenbrode, J. L., & Summons, R. E. (2021). A re-analysis of Murchison meteorite using tetramethylammonium hydroxide (TMAH) thermochemolysis under simulated sample analysis at Mars (SAM) pyrolysis GC-MS conditions. *Presented at the AGU Fall Meeting 2021, AGU*. Retrieved from https://agu.confex.com/agu/fm21/meetingapp.cgi/Paper/889062

Montgomery, D. R., Bandfield, J. L., & Becker, S. K. (2012). Periodic bedrock ridges on Mars. *Journal of Geophysical Research*, *117*(E3). https://doi.org/10.1029/2011JE003970

Murchie, S., Arvidson, R., Bedini, P., Beisser, K., Bibring, J.-P., Bishop, J., et al. (2007). Compact reconnaissance imaging spectrometer for Mars (CRISM) on Mars Reconnaissance Orbiter (MRO). *Journal of Geophysical Research*, *112*(E5), E05S03. https://doi.org/10.1029/2006JE002682

O'Connell-Cooper, C. D., Thompson, L. M., Spray, J. G., Berger, J. A., Gellert, R., McCraig, M., et al. (2022). Statistical analysis of APXS-derived chemistry of the clay-bearing Glen Torridon region and Mount Sharp group, Gale crater, Mars. *Journal of Geophysical Research: Planets*, *127*, e2021JE007177. https://doi.org/10.1029/2021JE007177

Palucis, M. C., Dietrich, W. E., Williams, R. M. E., Hayes, A. G., Parker, T., Sumner, D. Y., et al. (2016). Sequence and relative timing of large lakes in Gale crater (Mars) after the formation of Mount Sharp. *Journal of Geophysical Research: Planets*, *121*(3), 472–496. https://doi.org/10.1002/2015JE004905

Rampe, E. B., Blake, D. F., Bristow, T. F., Ming, D. W., Vaniman, D. T., Morris, R. V., et al. (2020). Mineralogy and geochemistry of sedimentary rocks and eolian sediments in Gale crater, Mars: A review after six Earth years of exploration with Curiosity. *Geochemistry*, *80*(2), 125605. https://doi.org/10.1016/j.chemer.2020.125605

Rampe, E. B., Bristow, T. F., Blake, D. F., Vaniman, D. T., Chipera, S. J., Downs, R. T., et al. (2022). Mineralogical trends over the clay-sulfate transition in Gale Crater from the Mars Science Laboratory CheMin instrument. *53rd LPSC*.

Rampe, E. B., Bristow, T. F., Morris, R. V., Morrison, S. M., Achilles, C. N., Ming, D. W., et al. (2020). Mineralogy of Vera Rubin ridge from the Mars Science Laboratory CheMin instrument. *Journal of Geophysical Research: Planets*, *125*(9), e2019JE006306. https://doi.org/10.1029/2019JE006306

Rampe, E. B., Ming, D. W., Blake, D. F., Bristow, T. F., Chipera, S. J., Grotzinger, J. P., et al. (2017). Mineralogy of an ancient lacustrine mudstone succession from the Murray formation, Gale crater, Mars. *Earth and Planetary Science Letters*, *471*, 172–185. https://doi.org/10.1016/j.epsl.2017.04.021

Rivera-Hernández, F., Sumner, D. Y., Mangold, N., Banham, S. G., Edgett, K. S., Fedo, C. M., et al. (2020). Grain size variations in the Murray formation: Stratigraphic evidence for changing depositional environments in Gale Crater, Mars. *Journal of Geophysical Research: Planets*, *125*(2), e2019JE006230. https://doi.org/10.1029/2019JE006230

Rudolph, A., Horgan, B., Johnson, J., Bennett, K., Haber, J., Bell, J. F., III, et al. (2022). The distribution of clay minerals and their impact on diagenesis in Glen Torridon, Gale crater, Mars. *Journal of Geophysical Research: Planets*, *127*, e2021JE007098. https://doi.org/10.1029/2021JE007098

Sanin, A. B., Mitrofanov, I. G., Litvak, M. L., Lisov, D. I., Starr, R., Boynton, W., et al. (2015). Data processing of the active neutron experiment DAN for a Martian regolith investigation. *Nuclear Instruments and Methods in Physics Research Section A: Accelerators, Spectrometers, Detectors and Associated Equipment*, *789*, 114–127. https://doi.org/10.1016/j.nima.2015.03.085

Seelos, K. D., Seelos, F. P., Viviano-Beck, C. E., Murchie, S. L., Arvidson, R. E., Ehlmann, B. L., & Fraeman, A. A. (2014). Mineralogy of the MSL Curiosity landing site in Gale crater as observed by MRO/CRISM. *Geophysical Research Letters*, *41*(14), 2014GL060310. https://doi.org/10.1002/2014GL060310

Stack, K. M., Dietrich, W. E., Lamb, M. P., Sullivan, R. J., Christian, J. R., Newman, C. E., et al. (2022). Orbital and in-situ investigation of periodic bedrock ridges in Glen Torridon, Gale Crater, Mars. *Journal of Geophysical Research: Planets*, *127*(6), e2021JE007096. https://doi.org/10.1029/2021je007096

Stack, K. M., Grotzinger, J. P., Lamb, M. P., Gupta, S., Rubin, D. M., Kah, L. C., et al. (2019). Evidence for plunging river plume deposits in the Pahrump Hills member of the Murray formation, Gale crater, Mars. *Sedimentology*, *66*(5), 1768–1802. https://doi.org/10.1111/sed.12558

Steele, A., McCubbin, F. M., Fries, M. D., Golden, D. C., Ming, D. W., & Benning, L. G. (2012). Graphite in the Martian meteorite Allan Hills 84001. *American Mineralogist*, *97*(7), 1256–1259. https://doi.org/10.2138/am.2012.4148

Sullivan, R., Baker, M., Newman, C., Turner, M., Schieber, J., Weitz, C., et al. (2022). The aeolian environment in Glen Torridon, Gale crater, Mars. *Journal of Geophysical Research: Planets*, *127*, e2021JE007174. https://doi.org/10.1029/2021JE007174

Summons, R. E., Amend, J. P., Bish, D., Buick, R., Cody, G. D., Des Marais, D. J., et al. (2011). Preservation of Martian organic and environmental records: Final report of the Mars biosignature working Group. *Astrobiology*, *11*(2), 157–181. https://doi.org/10.1089/ast.2010.0506

Thompson, L. M., Berger, J. A., Spray, J. G., Fraeman, A. A., McCraig, M. A., O'Connell-Cooper, C. D., et al. (2020). APXS-derived compositional characteristics of Vera Rubin ridge and Murray formation, Gale Crater, Mars: Geochemical implications for the origin of the ridge. *Journal of Geophysical Research: Planets*, *125*(10), e2019JE006319. https://doi.org/10.1029/2019JE006319

Thompson, L. M., Schmidt, M. E., Spray, J. G., Berger, J. A., Fairén, A. G., Campbell, J. L., et al. (2016). Potassium-rich sandstones within the Gale impact crater, Mars: The APXS perspective. *Journal of Geophysical Research: Planets*, *121*(10), 1981–2003. https://doi.org/10.1002/2016JE005055

Thompson, L. M., Spray, J. G., O'Connell-Cooper, C., Berger, J. A., Yen, A., Boyd, N., et al. (2022). Widespread alteration at the base of the Siccar Point unconformity and further evidence for regional, alkaline source rock(s) at Gale crater: Exploration of the Mount Sharp group – Greenheugh pediment cap rock contact with APXS. *Journal of Geophysical Research: Planets*, *127*, e2021JE007178. https://doi.org/10.1029/2021JE007178

Thomson, B. J., Bridges, N. T., Milliken, R., Baldridge, A., Hook, S. J., Crowley, J. K., et al. (2011). Constraints on the origin and evolution of the layered mound in Gale Crater, Mars using Mars Reconnaissance Orbiter data. *Icarus*, *214*(2), 413–432. https://doi.org/10.1016/j.icarus.2011.05.002

Thorpe, M. T., Bristow, T. F., Rampe, E. B., Tosca, N. J., Grotzinger, J. P., Bennett, K. A., et al. (2022). Mars Science Laboratory CheMin data from the Glen Torridon region and the significance of lake-groundwater interactions in interpreting mineralogy and sedimentary history. *Journal of Geophysical Research: Planets*, *127*, e2021JE007099. https://doi.org/10.1029/2021JE007099

Tu, V. M., Rampe, E. B., Bristow, T. F., Thorpe, M. T., Clark, J. V., Castle, N., et al. (2021). A review of the phyllosilicates in Gale Crater as detected by the CheMin instrument on the Mars Science Laboratory, Curiosity rover. *Minerals*, *11*(8), 847. https://doi.org/10.3390/min11080847

VanBommel, S. J., Gellert, R., Berger, J. A., Campbell, J. L., Thompson, L. M., Edgett, K. S., et al. (2016). Deconvolution of distinct lithology chemistry through oversampling with the Mars Science Laboratory Alpha Particle X-Ray Spectrometer. *X-Ray Spectrometry*, *45*(3), 155–161. https://doi.org/10.1002/xrs.2681

Vaniman, D. (2013). MSL Mars chemistry & mineralogy X-ray instrument 2 EDR V1.0 [Dataset]. NASA Planetary Data System. https://doi.org/10.17189/1519444

Vaniman, D. T., Bish, D. L., Ming, D. W., Bristow, T. F., Morris, R. V., Blake, D. F., et al. (2014). Mineralogy of a mudstone at Yellowknife Bay, Gale Crater, Mars. *Science*, *343*(6169), 1243480. https://doi.org/10.1126/science.1243480

Weitz, C. M., O'Connell-Cooper, C., Thompson, L., Sullivan, R. J., Baker, M., & Grant, J. A. (2022). The physical properties and geochemistry of grains on aeolian bedforms at Gale crater, Mars. *Journal of Geophysical Research: Planets*, *127*, e2021JE007061. https://doi.org/10.1029/2021JE007061

Wiens, R. C., Maurice, S., Barraclough, B., Saccoccio, M., Barkley, W. C., Bell, J. F., et al. (2012). The ChemCam instrument suite on the Mars Science Laboratory (MSL) rover: Body unit and Combined system tests. *Space Science Reviews*, *170*(1), 167–227. https://doi.org/10.1007/s11214-012-9902-4

Wiens, R. (2013a). MSL ChemCam laser induced breakdown spectrometer EDR V1.0 [Dataset]. NASA Planetary Data System. https://doi.org/10.17189/1519439 [Dataset]

Wiens, R. (2013b). MSL ChemCam remote micro imaging camera EDR V1.0 [Dataset]. NASA Planetary Data System. https://doi.org/10.17189/1519456

Williams, A., Eigenbrode, J., Floyd, M., Wilhelm, M. B., O'ReillyStewart, J., Johnson, S. S., et al. (2019). Recovery of fatty acids from mineralogic Mars analogs by TMAH thermochemolysis for the Sample Analysis at Mars wet chemistry experiment on the Curiosity rover. *Astrobiology*, *19*(4), 522–546. https://doi.org/10.1089/ast.2018.1819

Williams, A. J., Eigenbrode, J. L., Millan, M., Williams, R. H., Buch, A., Teinturier, S., et al. (2021). Organic molecules detected with the first TMAH wet chemistry experiment, Gale Crater, Mars. In *52nd Lunar and Planetary Science Conference, 1763*.

Wong, G. M., Franz, H. B., Clark, J. V., McAdam, A. C., Lewis, J. M. T., Millan, M., et al. (2022). Oxidized and reduced sulfur observed by the Sample Analysis at Mars (SAM) instrument suite on the *Curiosity* rover within the Glen Torridon region at Gale crater, Mars. *Journal of Geophysical Research: Planets*, *127*, e2021JE007084. https://doi.org/10.1029/2021JE007084

Wray, J. J. (2013). Gale crater: The Mars Science Laboratory/Curiosity rover landing site. *International Journal of Astrobiology*, *12*(1), 25–38. https://doi.org/10.1017/S1473550412000328

Yen, A. S., Ming, D. W., Vaniman, D. T., Gellert, R., Blake, D. F., Morris, R. V., et al. (2017). Multiple stages of aqueous alteration along fractures in mudstone and sandstone strata in Gale Crater, Mars. *Earth and Planetary Science Letters*, *471*, 186–198. https://doi.org/10.1016/j.epsl.2017.04.033